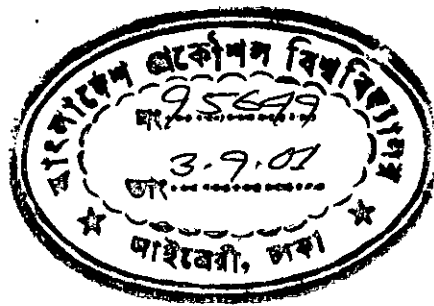
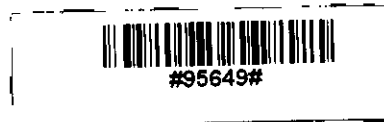


EFFECT OF COOLANT TEMPERATURE ON PERFORMANCE OF A SI ENGINE

BY
MOHAMMAD MAMUN



A THESIS
SUBMITTED TO THE DEPARTMENT OF MECHANICAL ENGINEERING
BANGLADESH UNIVERSITY OF ENGINEERING AND TECHNOLOGY (BUET)
IN PARTIAL FULFILLMENT OF THE REQUIREMENTS FOR THE DEGREE OF
MASTER OF SCIENCE IN MECHANICAL ENGINEERING.



BANGLADESH UNIVERSITY OF ENGINEERING AND TECHNOLOGY (BUET) DHAKA

AUGUST, 2001

EFFECT OF COOLANT TEMPERATURE ON PERFORMANCE OF A SI ENGINE

A Thesis

By


Mohammad Mamun

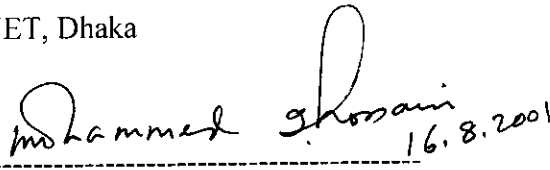
Submitted to the Department of Mechanical Engineering (BUET),

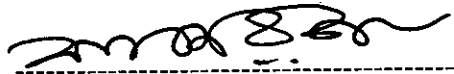
In partial fulfillment of the requirements for the degree of

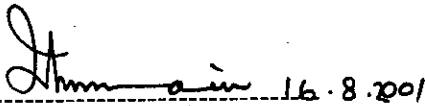
Master of Science and Engineering;

Approved as to style and contents:

1.  16.8.2001

Dr. Md. Ehsan
Associate Professor
Dept. of Mechanical Engineering
BUET, Dhaka
Chairman
2.  16.8.2001

Dr. Md. Imtiaz Hossain
Professor
Dept. of Mechanical Engineering
BUET, Dhaka
Member
3. 

Dr. M. A. Rashid Sarkar
Professor & Head
Dept. of Mechanical Engineering
BUET, Dhaka
Member (Ex- officio)
4.  16.8.2001

Prof A. K. M. Iqbal Hussain
Head, Energy & Environment Center
Islamic University of Technology
Board Bazar, Gazipur..

CANDIDATE'S DECLARATION

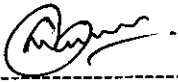
It is hereby declared that, this thesis or any part of it has not been submitted elsewhere for the award of any degree or diploma or publication.

Signature of the Supervisor:

Dr. Md. Ehsan
Associate Professor
Dept. of Mechanical Engineering
BUET, Dhaka

Supervisor

Signature of the Candidate:



Mohammad Mamun

Candidate

ACKNOWLEDGEMENT

This research work was conducted by the author under close supervision and thorough guidance of Dr. Md. Ehsan, Associate Professor, Department of Mechanical Engineering, Bangladesh University of Engineering and Technology (BUET). The author expresses his profound gratitude to his supervisor for his delicate supervision, ceaseless inspiration, deliberate encouragement and untiring support throughout this research work.

The author is also grateful to Dr. M. A. Rashid Sarkar, Professor and Head, Department of Mechanical Engineering, BUET, Dhaka, for his continuous pursuit of the developments at different stages of this research work.

The author remembers the assistance and cooperation of Mr. Nazmul Huda Al Mamun, Mr. Md. Nasim Hyder, Mr. Md. Hamidul Haque and Mr. Mohammad Zakir Hossain who helped during various stages of this work. He also thanks to the staff of the Heat Engine Laboratory, Mr. Md. Rukun Uddin for his continuous help during taking the readings.

Finally, the author would like to express his sincere thanks to all other teachers of the Mechanical Engineering Department, BUET and his friends who encouraged him during the research work and helps in the successful completion of the work.

ABSTRACT

This research work is aimed at investigating the effect of variation of coolant temperatures ranging from 45-85°C, thus effecting the heat removal rate, on the performance of an automotive SI engine. The specific aim of this study was to investigate the effect of variation of cooling water temperature as well as the cooling rate on the P-t and P-V diagrams of the engine cycle, at different speed and load conditions. A pressure transducer connected to the combustion chamber, signal conditioning hardware and a high-speed data acquisition device is used for recording cyclic variation of pressure. A position sensor tracks the TDC location as a time series, from which the cylinder volume is calculated using piston-cylinder dimensions. Performance parameters such as brake specific fuel consumption rate, air-fuel ratio, temperatures of coolant, lubricating oil as well as the engine body and emission analysis of the exhaust gases were also investigated at different engine speed and load conditions.

Investigations revealed that increased coolant temperature reduced the heat losses and resulted in slight improvement of specific fuel consumption. No significant change on the pressure-volume relationship was noticed. Variation of coolant temperature in this range did not change the combustion inside the cylinder very much, resulting in insignificant changes in exhaust temperature and emission analysis. The detrimental effects observed was the elevation of temperature of the engine parts and the lubricating oil. Although multi-grade lubricating oils appeared to be coping up with the rise of temperatures resulting in steady engine operation. Elevated body temperatures may have detrimental effect on the operational life of various non-metallic and metallic engine parts. When the coolant temperature was raised above 85°C the heat transfer and temperature rise became unstable due to local boiling and formation of vapour locks, leading to rapid engine overheating. This investigation may have practical implications when many automotive engines in Bangladesh are run with faulty/inadequate cooling systems specially in congested traffic jams in hot summer days.

CONTENTS

Title	0.1
Acknowledgement	0.4
Abstract	0.5
Contents	0.6
List of figures	0.8
List of graphs	0.9
Nomenclature	0.10

CHAPTER-1 INTRODUCTION

1.1 Introduction	1.1
1.2 Objectives	1.4

CHAPTER-2 LITERATURE REVIEW

2.1 Effect of Temperature on Engine Components and their Performance	2.1
2.2 Pressure as an Indicator of Engine Performance	2.3
2.3 Study of Emission from an Engine	2.4

CHAPTER-3 EXPERIMENTAL SETUP AND METHODOLOGY

3.1 The Experimental Setup	3.1
3.2 The Engine Test Bench	3.1
3.3 Pressure Transducer	3.2
3.4 TDC Position Sensor	3.3
3.5 Signal Conditioning Hardware	3.4
3.6 The Data-acquisition Hardware (ADC-11)	3.4
3.7 Exhaust Gas Emission Analyzer	3.6
3.8 Experimental Methodology	3.7

CHAPTER-4	EXPERIMENTAL RESULTS & DISCUSSIONS	
4.1	The Engine Performance	4.1
4.2	Variation of Specific Fuel Consumption	4.2
4.3	Variations in P-V Diagrams	4.3
4.4	Temperature Variations	4.8
4.5	Variations in Emission	4.9
CHAPTER-5	CONCLUSIONS AND RECOMMENDATIONS	
5.1	Conclusions	5.1
5.2	Recommendations	5.4
REFERENCES		R.1
APPENDIX – A	SPECIFICATIONS	
A.1	Petrol Engine and Test Bed	A.1
A.2	Pressure Transducer	A.2
A.3	Calibration of Pressure Transducer	A.3
A.4	ADC-11	A.4
APPENDIX – B	EXPERIMENTAL DATA	B.1

LIST OF FIGURES

- Fig.-3.1 Photograph of the Experimental Setup
- Fig.-3.2 Photograph of the Pressure Transducer
- Fig.-3.3 Pressure transducer adapter with spark plug
- Fig.-3.4 Schematic arrangement of the signal conditioning hardware
- Fig.-3.5 Photograph of an ADC-11 data acquisition hardware
- Fig.-3.6 Crypton 290 four channel gas analyzer
- Fig.-A2.1 Pressure transducer assembly for measuring in-cylinder pressure

LIST OF GRAPHS

- Fig.-1.1 Typical P-V diagram of an automotive SI Engine
- Fig.-4.1 Test engine performance at various speeds
- Fig.-4.2 Variation of bsfc at different loads with coolant temperature
- Fig.-4.3 Variation of A/F ratio at different loads with coolant temperature
- Fig.-4.4 Typical motoring cycle of an automotive engine at 315 rpm
- Fig.-4.5 Cyclic variation of P-V diagram, 2000 rpm and 27 hp
- Fig.-4.6 Pressure variation during suction and exhaust strokes, 3200 rpm
- Fig.-4.7 P-t diagram with TDC trigger at 2000 rpm and 19 hp
- Fig.-4.8 P-V diagrams at different coolant temperatures, 2000 rpm and 19 hp
- Fig.-4.9 P-V diagrams at different load conditions, 60°C
- Fig.-4.10 Variation of Lubricating oil temperature with coolant temperature
- Fig.-4.11 Variation of engine body temperature with coolant temperature
- Fig.-4.12 Variation of exhaust gas temperature with bhp at different coolant temp.
- Fig.-4.13 Variation of CO and CO₂ emission with coolant temp., (2000 rpm, 18 hp)
- Fig.-A3.1 Pressure vs. voltage diagram for the pressure transducer

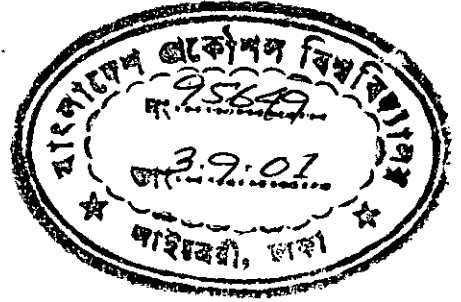
NOMENCLATURE

A/F	Air-Fuel
BDC	Bottom dead center
Bsfc	Brake specific fuel consumption
°C	Degree Celsius
°K	Degree Kelvin
cc	Cubic centimeter
CNG	Compressed Natural Gas
CO	Carbon monoxide
CO ₂	Carbon dioxide
g/kW-hr	Gram per kilowatt hour
HC	Hydrocarbon
hp	Horse power
Hz	Hertz
IC	Internal Combustion
IR	Infra-red
kW	Kilowatt
LPG	Liquefied Petroleum Gas
NG	Natural Gas
NO _x	Oxides of nitrogen
Ppm	Parts per million
Psi	Pounds per square inch
P-t	Pressure Time
P-V	Pressure Volume
Rpm	Revolution per minute
SI	Spark Ignition
TDC	Top dead center
Temp	Temperature
V	Volts
W	Watts

CHAPTER 1

INTRODUCTION

INTRODUCTION



1.1 Background

Temperature in the combustion chamber has always been an interesting research area for studying the effect on performance of IC engines. This is related to combustion parameters as well as the heat transfer rate to the cooling water. The coolant water may remove up to one third of the heat generated due to combustion that generally takes place at an optimized coolant temperature. This research work examines the use of in-cylinder measurements for engine control with emphasis on the analysis of cyclic variation of cylinder pressure (P-t) and Indicator Diagram (P-V) with coolant temperature along with other parameters such as Power developed, Brake specific fuel consumption rate, Air flow rate, Air-fuel ratio, Temperatures at intake and exhaust gases, Lubricating oil as well as the engine body and Emission analysis of the exhaust gases.

The P-V diagram is an important engine performance parameter. This represents the core of the cyclic variation of pressure inside engine cylinder which governs the net work done in a cycle and thus ultimately the indicated and brake power delivered by the engine.

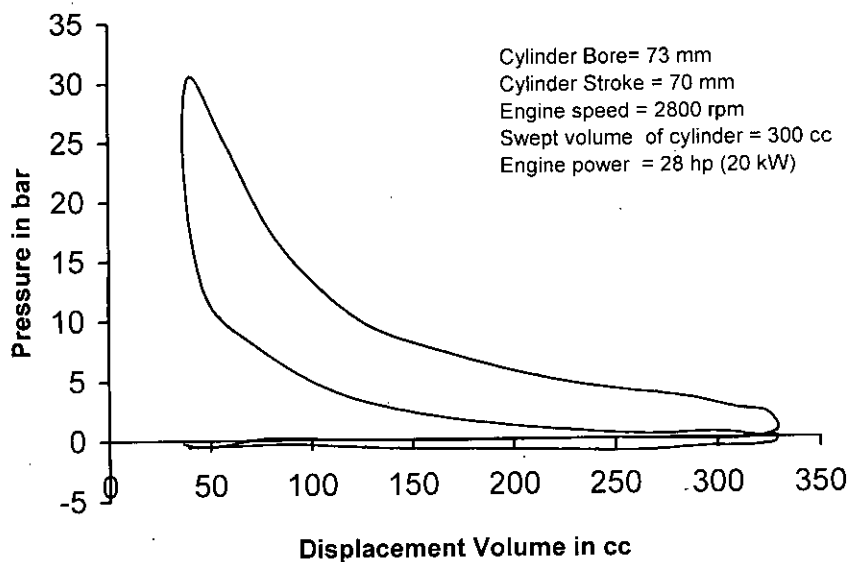


Figure-1.1 : Typical P-V diagram of an automotive SI engine.

Figure-1.1 shows the pressure-volume (indicator diagram) characteristics of a typical automotive spark ignition engine.

When the piston is at bottom dead center, the cylinder will have its largest volume. As the piston moves up the cylinder, the volume is reduced. At top dead center (TDC) the cylinder is at its minimum volume. The pressure reaches a peak (typically about 30-40 bar) when the cylinder reaches the TDC and the combustion has commenced. Following the trace of the cylinder pressure one can analyze problems and try changes in order to improve the power output from the engine. For example, as the piston moves down the cylinder during the power stroke, the pressure drops in the cylinder. This stroke is represented on the graph by the upper line that is swinging down and to the right from the peak pressure. Any changes that would result in a higher peak pressure and raise this segment of the line on the graph would result in more force pushing on the piston during the power stroke. In other words, the higher the pressure on graph during this segment the more power the engine can generate. The stroke is indicated by low pressure level as the piston moves to the left from the bottom dead center (BDC). In setting the valve timing the exhaust valve is opened at just the right time to make this pressure as low as possible.

When the piston moves up the cylinder, it has to push against that pressure during the exhaust stroke, using some of the power from the previous stroke. Once the piston reaches TDC on the exhaust stroke, it starts back down the cylinder for the intake stroke. If the intake manifold is restrictive, the volumetric efficiency is low and the pressure in the cylinder will drop (more vacuum) as the piston moves down the cylinder during the intake stroke. This is represented by lower pressure level as it moves back to the right during the intake stroke. Lower suction pressure requires more work to be done in bringing the piston down to the BDC during suction stroke. Finally the piston now moves back up the cylinder on the compression stroke. This is represented on the diagram by the pressure line swinging up the graph as the piston moves back to the TDC. Near the end of the compression stroke, the ignition starts the combustion, at this point the pressure rises sharply and heads up to the peak pressure again.

P-V Diagram allows us to intricately examine the impact of various parameters e.g. ignition timing, valve timing, coolant temperature, combustion temperature and intake and exhaust manifold design modifications. With improvements in sensor technology and the advent of cheap, reliable powerful digital signal processors, the hurdles to acquire and use the cylinder pressure and other high-bandwidth signals have become easier. These signals are used for performance diagnostics and engine control.

The parameter chosen in this investigation was the temperature of the cooling water of the engine on its way back to the radiator. The coolant water outlet temperature was varied through 45-85°C by adjusting the water flow. So heat losses to the cooling water was rather controlled qualitatively (lower mass flow and higher temperature difference), rather than quantitatively. On the other hand the elevated water temperature in the water-jacket could have quantitatively influence the combustion process and heat losses to some extent.

This investigation may have practical implications when many automotive engines in Bangladesh are run with faulty/inadequate cooling system specially in congested traffic jams in hot summer days. It may also contribute to indicate the causes of emissions from the engine. From technological point of view, this project for high speed computerized data acquisition of the indicator diagram (P-V) would be one of the first of its kind in our country and it could open up an enhanced arena for further investigation of the various other parameters related to the engine performance.

1.2 Objectives

The present research work has the following main objectives:

- (i) To study the performance of an water cooled automotive SI engine for the following parameters at a particular load and speed condition.
 - (a) Pressure-Time (P-t) and Pressure-Volume (P-V) traces using high speed data acquisition system.
 - (b) Power developed and Brake specific fuel consumption rate.
 - (c) Air-fuel ratio.
 - (d) Temperatures at coolant outlet, lubricant, intake and exhaust gases as well as the engine body.
 - (e) Emission analysis of the exhaust gases.
- (ii) Repeating the performance test for a number of different cooling water flow rates resulting in different water outlet temperatures, while the cooling water inlet temperature is kept constant.
- (iii) Repeat the set of tests mentioned in (i) and (ii) with a number of different speed and load conditions, covering the entire working range of the engine.

CHAPTER 2

LITERATURE REVIEW

LITERATURE REVIEW

2.1 Effect of Temperature on Engine Components and their Performance

Combustion temperatures are in the neighborhood of $2,500^{\circ}$ K in a spark-ignition engine, and the exhaust gas temperature is about $1,300^{\circ}$ K [Lumley 1999]. On the other hand, the melting point of aluminum is about 933° K and the melting point of iron is about $1,808^{\circ}$ K. It is clear that some provision has to be made to keep the piston, valves, and cylinder walls cool, or they will melt. Even considerably short of melting, at high temperatures metals begin to lose their strength, and this must also be avoided. Any heat removed represents a loss of energy, so we want to cool only as much necessary to maintain the strength of the materials, maintain clearances, and prevent the lubricant from breaking down.

The temperature profiles inside the combustion chamber have revealed concentration of high temperature zone in-between the inlet and the exhaust valves [Finlay et. al. 1985, French et. al. 1973]. The problem areas are the exhaust valve and the piston crown. The exhaust valve head loses most of its heat to the valve seat (the amount lost to the valve guide is relatively small, because the path is long and the conduction area is small). Unfortunately, when the valve opens, it is exposed to the exhaust gases, which flow past it at high velocities (facilitating heat transfer), and while this is happening the valve head is not in contact with its seat.

In water-cooled engines the water returning from the radiator, which therefore has the lowest temperature, usually flows around the cylinders and then up into the cylinder head. This is not the most effective order because the cylinder heads, and particularly the valve seats, require cooling much more than the cylinder walls. At say, $1,000^{\circ}$ K, the valve material has lost a substantial fraction of its strength. However, this method of cooling is adequate, and cheap. A supercharged engine with a small number of large cylinders,

running at high speed, will be likely to have a cooling problem. It is clear that two small exhaust valves will run cooler than one large one.

The piston crown is exposed to the gases at combustion temperatures, as is the wall of the combustion chamber. However, the combustion chamber wall has the cooling water on the other side (or the cooling fins in the case of an air cooled engine). The piston crown usually does not have any cooling on the under surface (although it may have oil or water jets. Any heat absorbed by the crown must be conducted to the sides of the piston in contact with the cylinder walls, and this path is relatively long. This contact with the cylinder wall is not good from a heat transfer point of view, since through most of the cycle there is no metal-to-metal contact (the surfaces are separated by a thin oil film) and the contact area is small, but the path length is the major factor. The temperature of an aluminum piston is considerably closer to the sink temperature than that of a cast iron piston. Cast-iron pistons are reported to run 40°K-80° K hotter than aluminum pistons [Heywood 1988].

Investigation of effect of coolant temperature on combustion chamber has revealed spark timing as an important phenomena [French et. al. 1973]. It justifies that a cooler head permits greater spark advance (in cooler gas, the auto-ignition reaction is slower to go to completion, so that the end gas is burned before it autoignites), and warmer cylinder bores (within limits) give lower ring friction. However, data on heat transfer from local areas in the cylinder (e.g., exhaust valves, piston crowns) are relatively sparse and have a lot of scatter. The total heat lost to the water jacket from the cylinder is defined in terms of overall engine heat transfer coefficient by $Q = A_p h (T_g - T_c)$, where Q is the heat lost from the gases per unit time, A_p is the piston area, T_g is the cycle mean gas temperature, and T_c is the mean coolant temperature [Taylor 1966]. These are clearly quantities that are easy to measure, although not precisely the most meaningful ones. For example, we would expect that the heat transfer would depend on the total surface area in the cylinder; however, it is reasonable to expect that this will be roughly proportional to the piston area. Also, the heat lost should be proportional to the difference between the gas temperature and the wall temperature, but since most engines have similar construction, the

temperature difference between the gas and the wall will usually be roughly the same fraction of the difference between the gas and the coolant. Increasing the compression ratio in an SI engine have been reported to decrease the heat flux to the coolant up to certain limit [Kerley et. al. 1962].

2.2 Pressure as an Indicator of Engine Performance

As early as 1951, cylinder pressure was proposed as a feedback signal for use in a closed-loop ignition control scheme [Draper et. al.1951]. It is shown that a specific crank-angle location of peak pressure correlates well with best torque, and can be used for closed loop control of ignition timing [Powell et. al. 1983]. It is proposed to use the combustion phasing angle, defined as the crank angle where apparently 50% of the heat from the combustion process in a cycle has been released, for Maximum Brake Torque (MBT) ignition timing [Klimstra 1985].

Different methods of measurement of peak cylinder pressure are practiced [Jacobson et. al. 1999]. Quantitative analysis of the pressure signal has been proposed for estimation and closed-loop control of air-fuel ratio. Using regression techniques correlated cylinder pressure measurements with AFR, EGR rate, HC, NO_x, CO and CO₂ emissions [Wibberley et. al. 1989]. A single-zone combustion model is used to regulate position of an equivalent heat release, which resulted in an indirect control of AFR [Leisenring et. al. 96].

Studies have also been made recently to correlate the estimation of heat release rate with cylinder pressure data using quantitative analysis approach [Tunestal et. al. 1998]. The author demonstrated that relatively computationally intensive tasks can be performed easily on a cycle by cycle basis and the results fed back to an engine controller. They also suggest to investigate the influence of spark timing and air-fuel ratio on these pressure-based parameters, and further, on exhaust composition and temperature, since this is what determines the tailpipe emissions and time to light-off the catalytic converter.

2.3 Study of Emission from an Engine

In production of oxides of nitrogen, IC Engines are about on a par (47%) with other sources; in production of hydrocarbons it is a little below other sources, at 39%, while in production of carbon monoxide it is the major source at 66%; in production of carbon dioxide, it is responsible for something like 14% of fossil fuel burning worldwide [Greene et. al. 1993]. The IC Engines have has several features that make it essential to control. Automobiles are everywhere, and are close to the ground, so they constitute a distributed lowlevel source. Particularly in urban areas, this distributed pollution is difficult for the atmosphere to remove. In addition, where there are cars, there are people, so that the pollution is associated with high population density, the worst possible situation. If this is combined with an unfortunate atmospheric and geographic situation that tends to confine the pollution, and prevent its being washed away by the weather, we have a recipe for disaster.

There are several things that can be done to alleviate CO₂ production by the automobile. Fuel consumption could be substantially cut with engines of the current type if the vehicle were much lighter. The majority of fuel consumption is spent in acceleration (and then dissipated to heat when the vehicle is braked). A much lighter vehicle could run with a much smaller engine and still have interesting performance. Drag coefficients could be cut approximately in half, at most [Hucho et. al. 1993, Committee on Fuel Economy Tech. Rep.1992], although a factor of 2/3 is probably more realistic; this would reduce fuel consumption at higher speeds. High fuel economy prototype vehicles, which are mostly quite light, and some of which have low drag coefficients, have fuel consumptions in the neighborhood of 3-4 L/100 km [Committee on Fuel Economy Tech. Rep.1992]. Space-age plastics and aluminum are beginning to be used in automobile construction and can help to reduce total vehicle weights considerably.

The NO_x production is primarily a function of temperature. The adiabatic flame temperature peaks for mixtures slightly richer than stoichiometric, and falls for both fuel-rich and fuel-lean, even for gaseous hydrocarbon fuels.

Unburned hydrocarbons are produced in the cylinder primarily from the quenched regions between the piston and the cylinder wall, above the top piston ring, as well as inside the spark plug, around the valves and in corners; that is, regions that are surrounded by too much chilled surface area, so that their temperature is reduced below the point of ignition. Roughly 9% of the fuel entering the cylinder escapes normal combustion [Cheng et. al. 1993]. About 4.5% (about half) of this escaped fuel is oxidised later in the expansion, but only about 1/4 of this contributes to the imep (because the oxidation takes place when the pressure and temperature have fallen). The other 4.5% is not oxidised in the cylinder. Some of this is recycled (as residual gases or as blowby). Of the part that goes into the exhaust, about one-third is oxidised in the exhaust port and manifold. Finally, between 1.5% and 2% (say, 1.8%) remains. Of this, half is unburned fuel and half is partially reacted fuel components.

CO is a product of incomplete combustion. In an abundance of oxygen, CO would combine with the O_2 to form CO_2 . Hence, when there is an excess of oxygen (lean) there is relatively little CO produced. As the mixture gets richer, so that there is less and less oxygen available, the amount of CO produced increases. Again, this has partly to do with the poor mixing of the charge. The same effect would happen in a perfectly mixed reactor. However, here it is exaggerated somewhat because the richest regions in the poorly mixed charge produce disproportionately more CO. The upper and lower air:fuel mass ratios for ignition of gasoline in air are approximately 42.8 and 3.2 [Adler et. al. 1993]. However, ignition of a mixture substantially leaner than stoichiometric is not reliable. The ignition limit means that a mixture leaner than 42.8 is essentially impossible to ignite, but an engine will run only very unevenly, with many misses, at mixtures well beyond stoichiometric toward the lean limit.

But even under very lean operating conditions, the engine still produces NO, CO and unburned hydrocarbons. However, thermal efficiency is improved in lean burn for several reasons: the exhaust gases have a composition much closer to air, and a lower temperature, and both of these increase the specific heat; the induction of excess air reduces the pumping losses; heat loss is reduced because the exhaust gas temperature is lower [Kim et. al. 1994]. Effect of cooling rate has also been investigated from exhaust emission point, specially for cold starting conditions. Reducing surface temperature of combustion chamber has shown very limited effect on HC emissions [Frank et. al. 1991].

CHAPTER 3

EXPERIMENTAL SETUP AND METHODOLOGY

EXPERIMENTAL SETUP AND METHODOLOGY

3.1 The Experimental Setup

The experimental setup for this project work consisted of the following main features:

- Standard engine test bed with proper instrumentation for measurement of engine power, speed, flow rate of – fuel, water and air, as well as relevant temperatures.
- A pressure transducer connected to the combustion chamber.
- A position sensor for tracking the TDC location as a time series, from which the cylinder volume is calculated using piston-cylinder dimensions.
- Signal conditioning hardware.
- A high-speed data acquisition device for recording cyclic variation of pressure.
- An apparatus for emission analysis of exhaust gas.

3.2 The Engine Test Bench

The standard engine test bed was equipped with necessary instrumentation for measurement of engine performance. A typical automotive spark ignition engine (1171 cc, NISSAN, 4-cylinder, 4-stroke, water cooled) was mounted on the tested bed. Detailed specification of the engine tested is given in appendix-A.1. A water brake dynamometer was coupled with the engine using a universal joint. Dynamometer was equipped with load changing facilities using water flow control and adjusting the impeller angles. A calibrated load cell with digital display was used to measure the torque. A magnetic pick-up transducer with digital display was used for engine speed measurement. Air flow rate was calculated from a depression measured across a orifice in the suction line. Cooling water flow rate was measured using a calibrated flow meter. A graduated measuring flask was used to measure the fuel consumed volumetrically in a time period measured using a stopwatch. Resistance temperature detectors (RTD) were provided to measure the temperatures of - cooling water at engine inlet and outlet, intake air and exhaust gases, lubricating oil and engine body (spark plug seat). Figure-3.1 shows a Photograph of the Experimental Setup which includes the Engine Test Bench with control and display panel, Oscilloscope, Signal Conditioning Devices, Computer and Emission Analyzer.

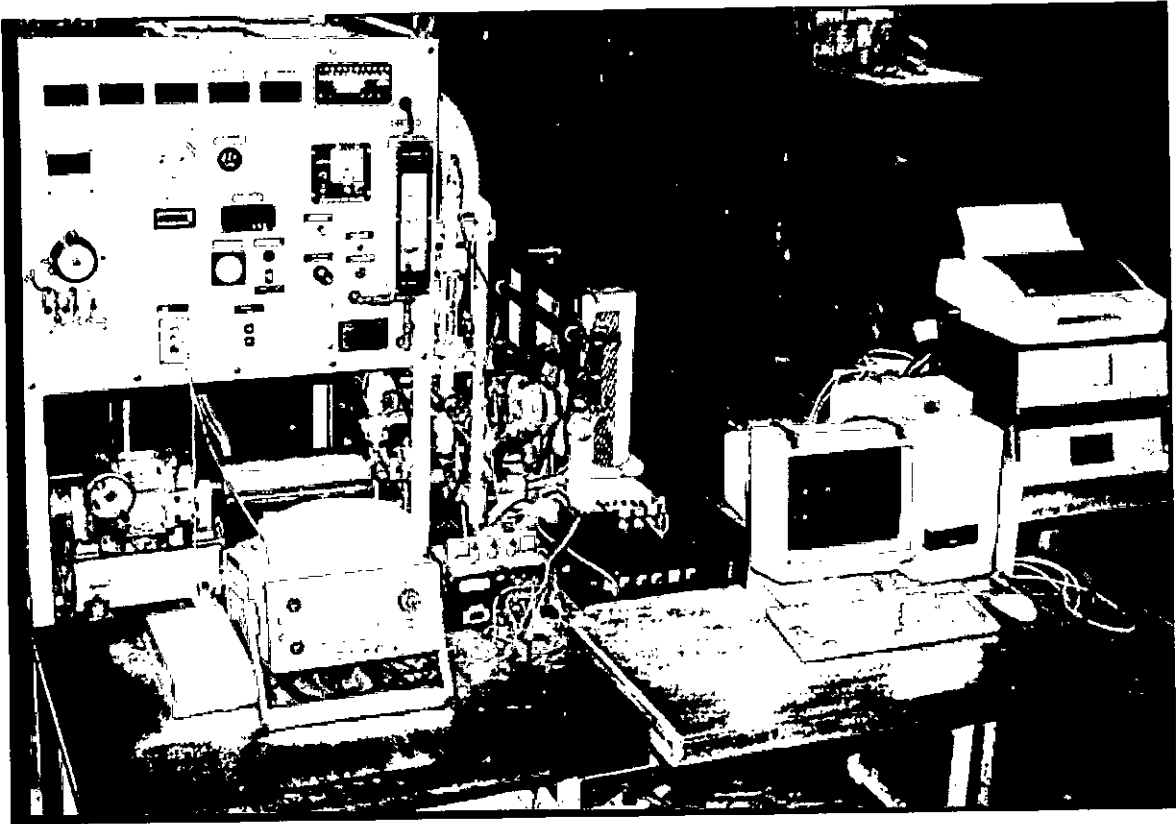


Figure-3.1 : Photograph of the Experimental Setup

3.3 Pressure Transducer

An engine cylinder pressure measuring transducer was used for surveying alternative cylinder pressure in succession. The pressure signal was used to generate P-V diagram and the P-t diagram of the cycles. Figure-3.2 shows photograph of the pressure transducer.

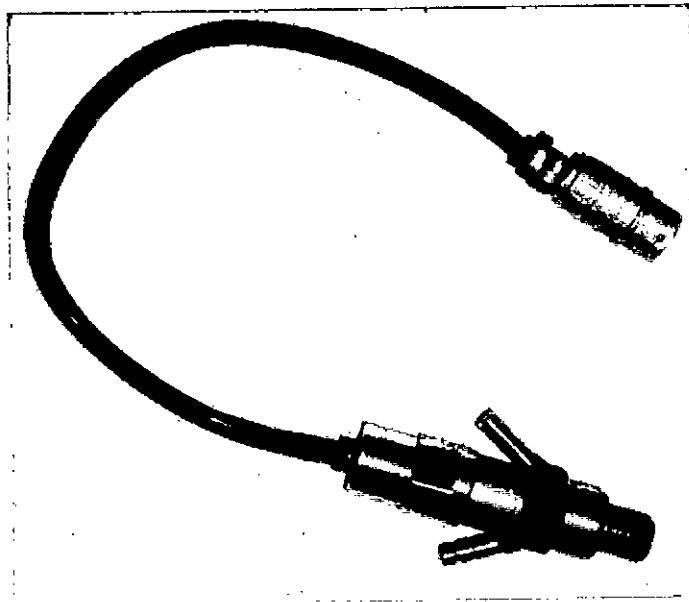


Figure 3.2 : Photograph of the Pressure Transducer.

The pressure transducer was attached to the engine cylinder through the spark plug hole using a special adapter as shown in figure-3.3. A small supply of cooling water is used to protect the piezo-electric pressure transducer from the heat of the combustion gases. The pressure transducer had a range of about 50 bars with a natural frequency of 40 kHz. Detailed specification of the transducer is given in appendix A.2.

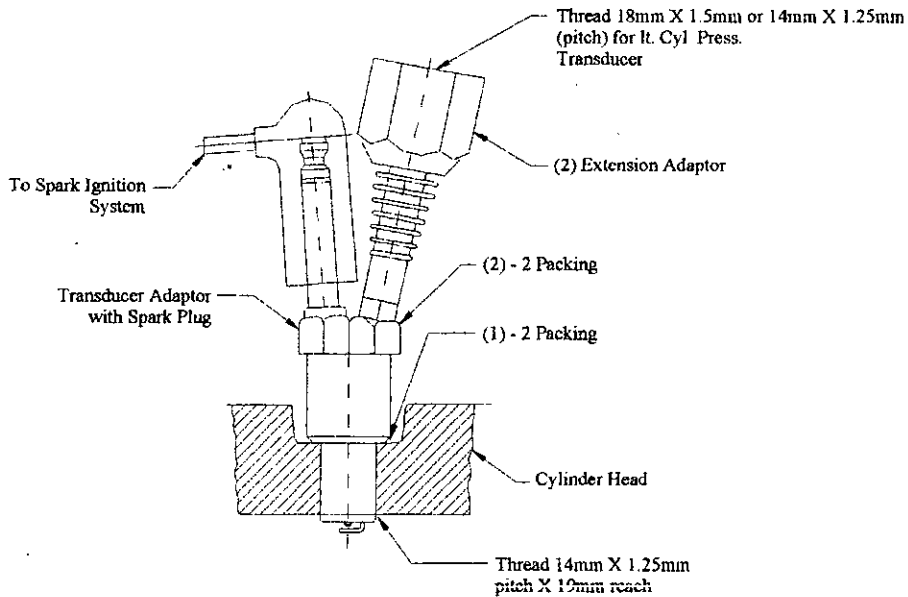


Figure-3.3 : Pressure transducer adapter with spark plug

3.4 TDC Position Sensor

An inductive type TDC detector (proximity switch) was provided to send a trigger signal, whenever the cylinder, in which the pressure transducer have been attached, reaches the top dead center. A mechanical part precisely attached to the flywheel (in accordance to the TDC position) causes the proximity switch to generate a signal, whenever it passes by it. For optical identification a LED was connected in parallel to the signal, which provided a light output indicating the TDC position. From the time series of TDC signals recorded the corresponding cylinder volume change was calculated using standard geometrical relationship of crank-piston mechanism, involving the stroke and crank radius dimensions.

3.5 Signal Conditioning Hardware

The signal from pressure transducer was in the order of mili-volts and it needed conditioning before it could be recorded by the data-acquisition hardware. Basically the hardware circuits had two components. The first was the amplification and filtering circuit and second component protected the computer from any undesirable voltages from the transducer. The acceptable range of the data-acquisition hardware was 0-2.5 volts DC as an input. The signal from the TDC detector collected across the indicating LED was about 1 volt in value and hence could be used without amplification.

The signal amplification circuit mainly used operational amplifiers and filter circuits. This unit was equipped with variable gain facility and needed to be supplied with a +15v and – 15v regulated DC supply. A precision voltage simulator ranging 0-2.5 volt was also built to provide a zero-adjustment signal for the voltage amplification circuit. The output of the amplification circuitry for the pressure signal was calibrated against a dead weight pressure gauge tester. The calibration curve is given in appendix-A.3. This allowed the voltage signal recorded by the data-logger to be converted to corresponding pressure values. For protection of the data-acquisition hardware and the computer from any undesirable voltage from the test bench or engine side a voltage limiting circuit using zenar-diode was used for both of the intake signals. Figure 3.4 shows the schematic arrangement of the signal conditioning hardware working between the transducers and the data-acquisition hardware mounted on the parallel port of the computer. The present voltage limiter board using zenar-diode circuits can handle up to five channels at a time.

3.6 The Data-acquisition Hardware (ADC-11)

ADC-11 is a parallel port mounted eleven channel data-acquisition hardware. This device was used for the high speed data-acquisition of the pressure and TDC position sensor. Input voltage range is 0-2.5 volts DC with a maximum resolution of 10 bits and a maximum sampling rate of 15,000 samples per second. Because the input signals from the transducers are analogue ones the need to be digitized before the computer (which only understands digital signals of 1 and 0) can handle them. This requires an analogue to digital signal converter. ADC-11 has a built-in highly compact 10 bit analog to digital converter and noise filtering electronics and it can be connected to the parallel port through common 25 pin D-connector.

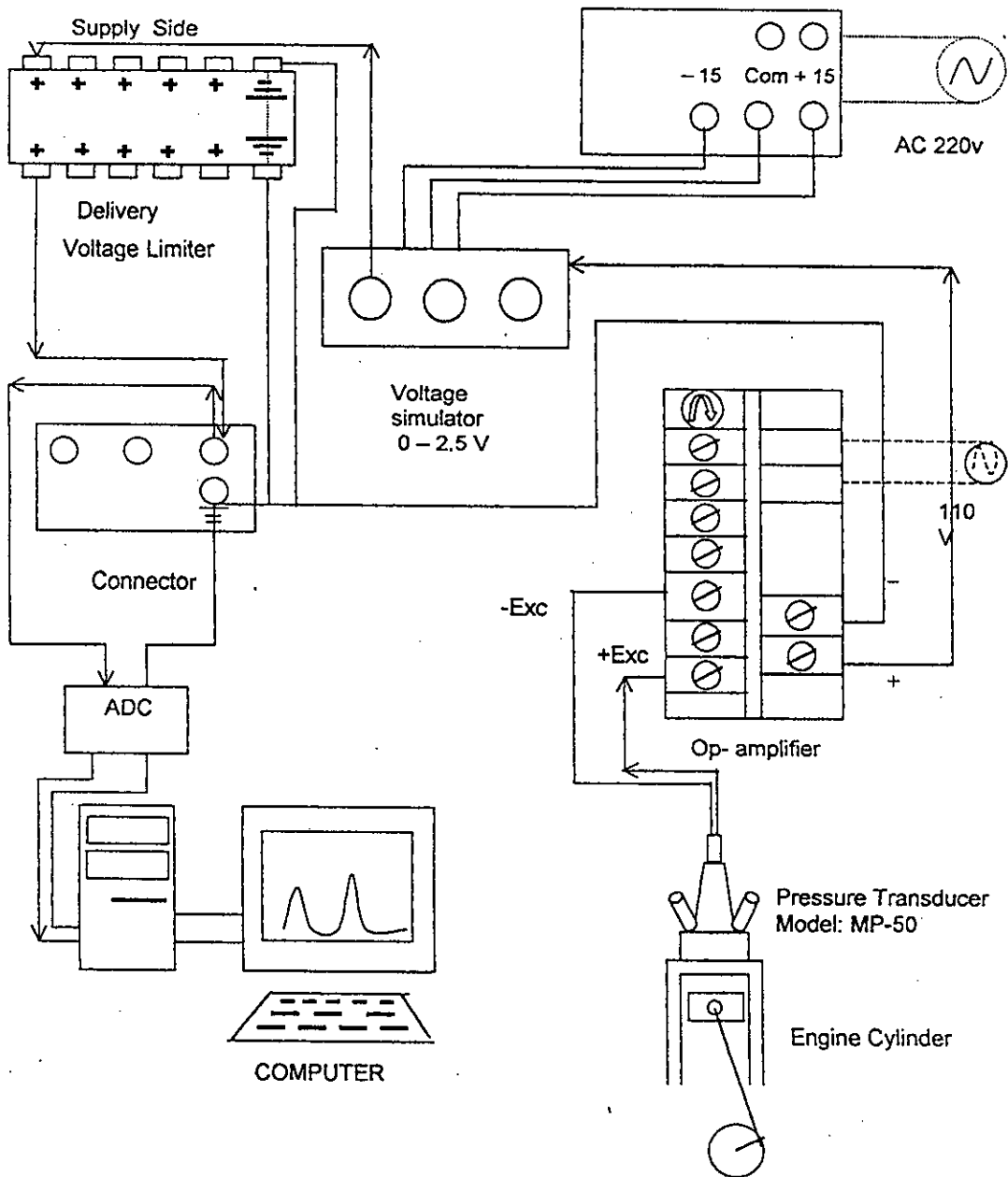


Figure 3.4 : Schematic arrangement of the signal conditioning hardware

The detail specification of the ADC-11 data-acquisition hardware is given in appendix A.4. Figure-3.5 shows the photograph of a ADC-11 almost at the true scale.

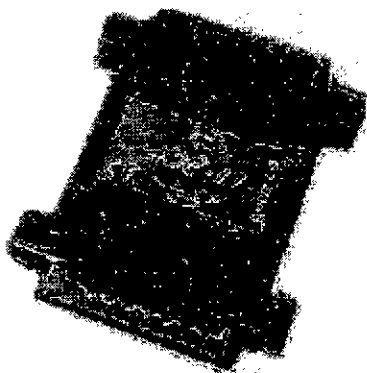


Figure-3.5 : Photograph of an ADC-11 data acquisition hardware

ADC-11 is also provided with two software programs PICOSCOPE and PICOLOG, both of them available in Windows and DOS version. PICOSCOPE is used for high-speed data-acquisition, which practically turns the computer monitor into a real-time oscilloscope. It has the capability of showing up to four signals simultaneously with the added advantage of very easy transfer/storage of data to the computer disc in standard format usable by other common database and mathematical software. The PICOLOG software is used for data logging at slower rates (e.g. only several times in second or more) and hence was not used in this investigation. Moreover, to verify the signals recorded by ADC-11, the P-t series was simultaneously monitored in a conventional CRT oscilloscope, which showed good agreement.

3.7 Exhaust Gas Emission Analyzer

A 4-gas emission analyzer (CRYPTON 290) was used to measure the proportion of different gas components of the exhaust emissions. Measurements from the emission analyzer showed percentage of Oxygen (O_2), Carbon-di-oxide (CO_2) and Carbon-monoxide (CO); Total Hydrocarbon (HC) in ppm, equivalence ratio of the intake air-fuel mixture and rpm of the engine. The analyzer passes infra-red (IR) light through exhaust samples collected by the built-in pump, for CO_2 , CO and HC measurements, while a chemical O_2 sensor cell is used to determine the proportion of O_2 . The system is automatically calibrated with respect to atmospheric air and hence does not need any calibration gas frequently. The air-fuel ratio is calculated using a stoichiometric value for the fuel used (14.7 for unleaded petrol/octane and 17.3 for NG). For the measurement of the engine speed a inductive probe was used which sensed the sparking rate reaching the spark plug. All the displayed readings were printed directly to a printer. It should be noted that CRYPTON 290 requires an initial warm-up period of about five minutes. Figure 3.6 shows the photograph of the emission analyzer used.

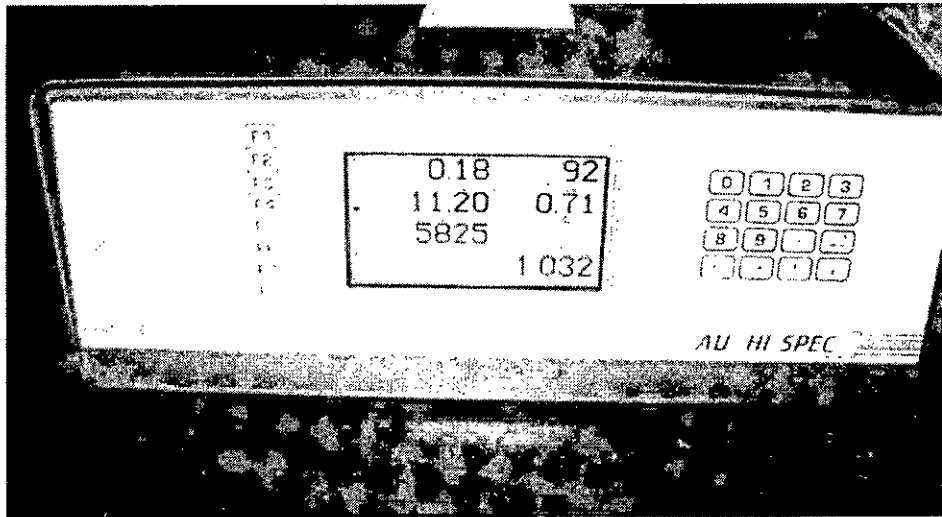


Figure 3.6 : CRYPTON 290 four channel gas analyzer

3.8 Experimental Methodology

- (i) Performance study of the engine at a particular load and speed for the engine parameters mentioned above keeping the cooling water outlet temperature at 45 °C by coolant flow adjustment through a regulating valve. Performance tests are carried out on standard engine test bench which is equipped with RTD sensors for temperature measurement. A CRYPTON 290 four-channel exhaust gas analyzer (CO₂, CO, HC, O₂) is used for emission analysis.
- (ii) Repeating the test for the same engine load and speed, for coolant water outlet temperatures of 60, 75 and 85°C respectively, while the inlet water temperature remains the same.
- (iii) Repeating this set of tests (with a series of outlet water temperatures), for different engine load and speed conditions covering the entire working range of the engine. For this the speed vs. power curve given by the engine manufacturer will be followed.
- (iv) Specifically compare the P-t and P-V diagrams with different coolant temperatures at different engine load and speed conditions. A pressure transducer connected to the combustion chamber, signal conditioning hardware and a high-speed data acquisition device is used for recording cyclic variation of pressure. A position sensor tracks the TDC location as a time series, from which the cylinder volume is calculated using piston-cylinder dimensions.

CHAPTER 4

EXPERIMENTAL RESULTS AND DISCUSSIONS

EXPERIMENTAL RESULTS AND DISCUSSIONS

4.1 The Engine Performance:

The engine was tested at a number of speed and load conditions covering its entire working range. The 1.2 liter, 4-stroke, 4-cylinder, water-cooled automotive SI engine had a rating of maximum 30 hp at a speed of 3200 rpm. Figure-4.1 shows the variation of standard engine power and torque as measured with increased engine speeds. Tests were carried out at speeds of 1600, 2000, 2400, 2800 and 3200 rpm. BS5514 was used as the derating standard and the results closely resemble the performance curve supplied by the engine manufacturer.

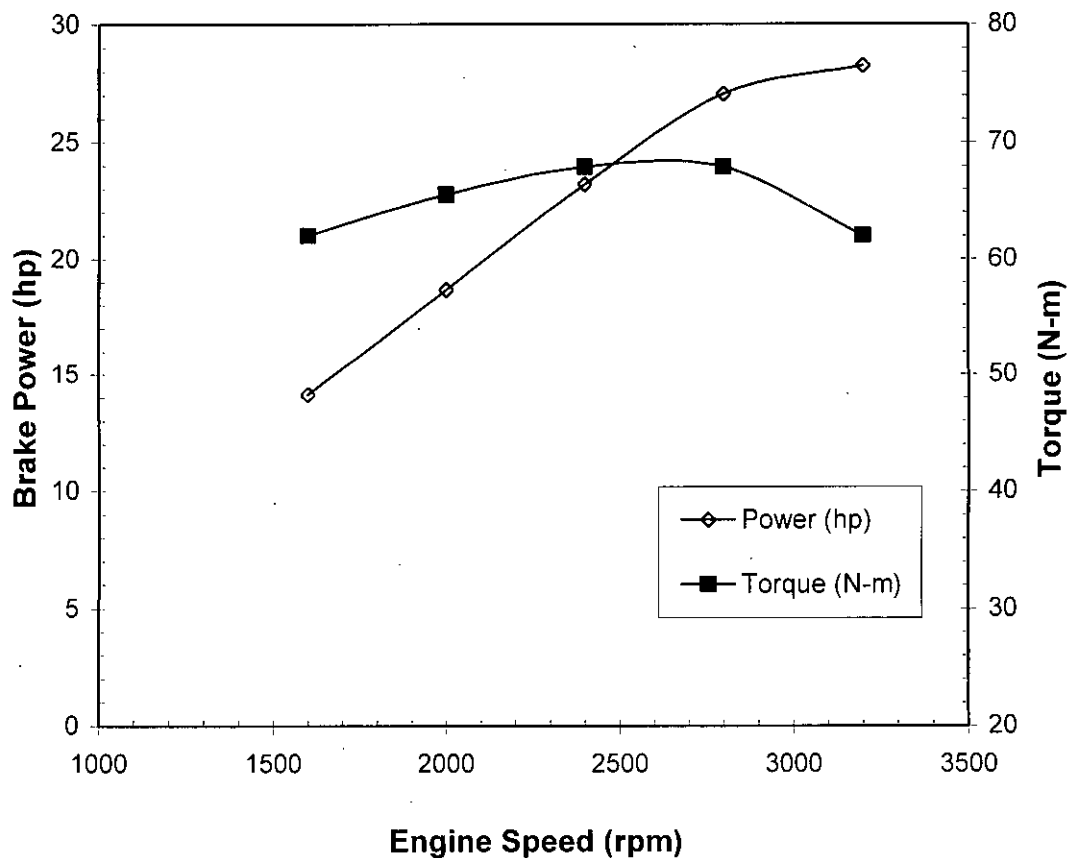


Figure-4.1 : Test engine performance at various speeds.

4.2 Variation of Specific Fuel Consumption

The variation in bsfc with engine load for various coolant temperatures are shown in figure-4.2. For all coolant temperatures the brake specific fuel consumption rate improves as the engine runs from part load to full load. As the cooling water outlet temperature is increased from 45°C to 85°C small improvement of bsfc (about 1-2%) was noticed. Small reduction in heat losses to cooling water mainly is responsible for this change. The small reduction in the fuel consumption rate slightly effects the air-fuel ratio as shown in figure-4.3, which is also supported by emission analyzer readout.

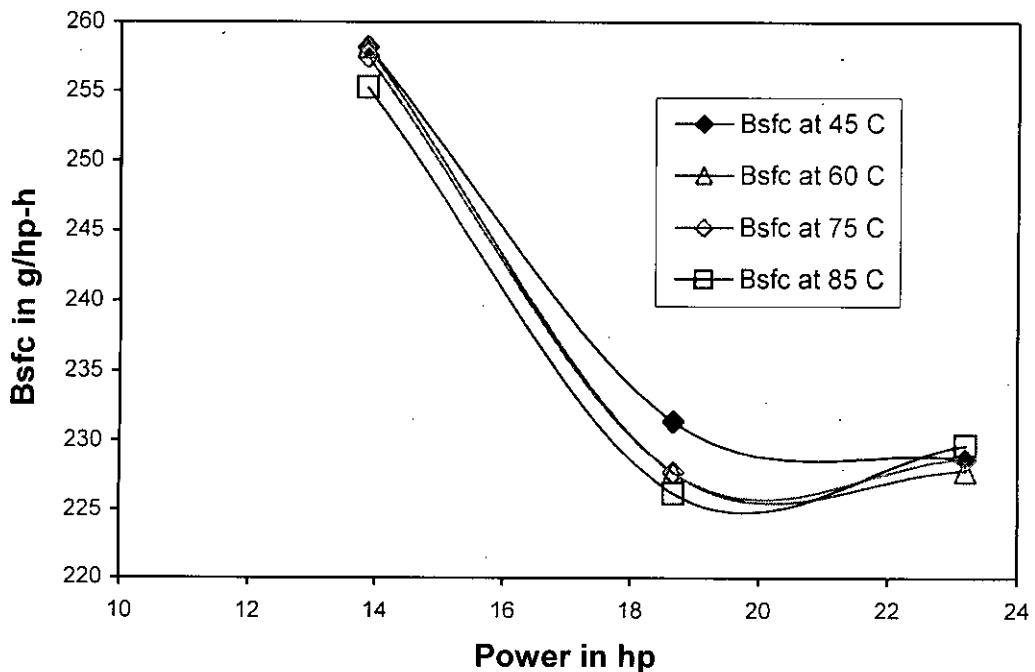


Figure-4.2 : Variation of Bsfc at different loads with coolant temperature.

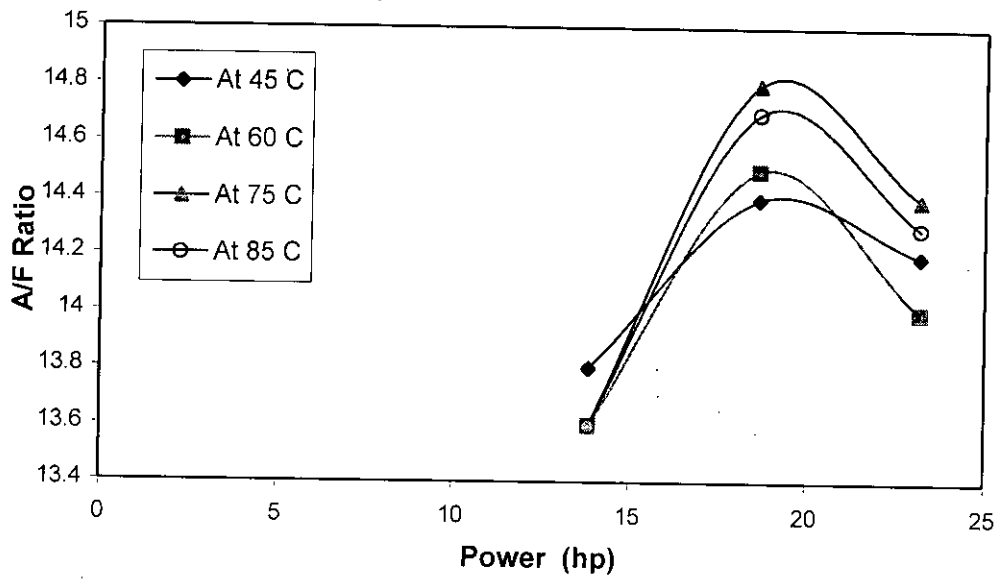


Figure-4.3: Variation of A/F Ratio at different loads with coolant temperature.

4.3 Variations in P-V Diagrams

At the first phase of the data acquisition the motoring cycle of the engine was recorded at about 300 rpm. Although this had no significance in the present study, it was an interesting and useful experience for verifying the results recorded. Figure 4.4 shows a typical motoring cycle of the test engine.

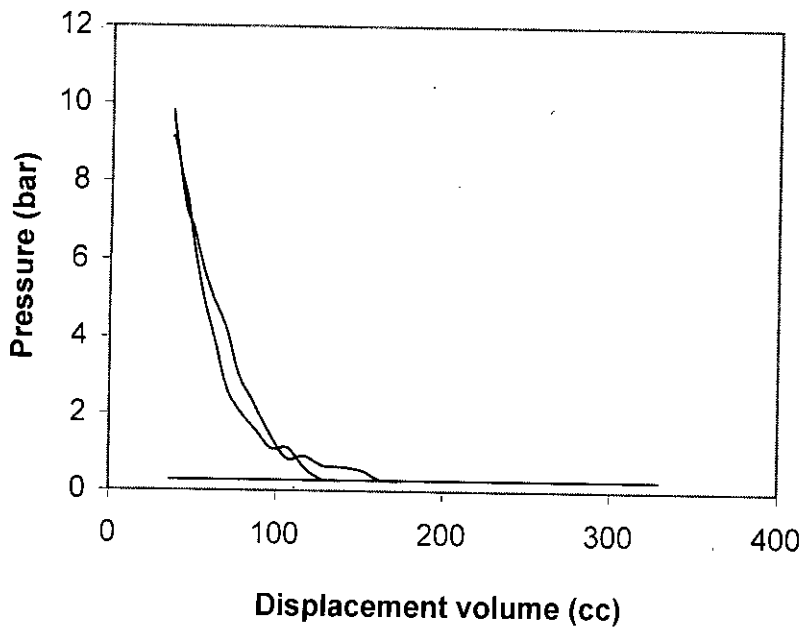


Figure-4.4: Typical motoring cycle of an automotive engine at 315 rpm.

At each of the tested power levels the P-V diagram showed cyclic variation in the peak pressure level attained almost randomly, but the variation was within $\pm 10\%$ of the peak value. This is a common feature in high-speed engines but due to the facts that - the peak pressure is only available in small fraction of the cycle, effects of multiple cylinders and the flywheel; this does not change the average output significantly. Figure-4.5 shows cyclic variation of peak pressure valued at different speed and load conditions.

Pressure fluctuations were observed in the low pressure-levels also (suction and exhaust strokes). Such details as shown in figure-4.6 are only visible when plotted at low pressure scales. These are due to the opening and closing effect of the intake and the exhaust valves. The corners of the P-V diagrams are also rounded (instead of sharp corners of the ideal Otto cycle) as valves can not open/close instantly. It rather happens gradually and it takes some time.

Figure 4.7 shows the P-t diagram with TDC trigger at 2000 rpm and 19 hp. The cycle time is determined by any three adjacent (consecutive) trigger marks in the diagram. For example, the cycle 2 is represented by the three adjacent trigger marks that represent 120 miliseconds (60 to 120 in the time axis) for the cycle duration.

With the change of coolant temperature no significant change in the P-V diagram was observed. This was true for all load conditions, indicating not much change in the cyclic pressure or work done. Figure 4.8 shows the variation of pressure-volume diagrams for different coolant temperatures with engine running at 2000 rpm producing about 19 horse power.

Figure 4.9 shows the gradual increment of the P-V diagram area at different speeds with a coolant temperature of 60°C . The P-V diagrams does not appear vastly different due to the torque characteristics of the engine, but the power output varies widely due to the difference of cycle repeating frequency.

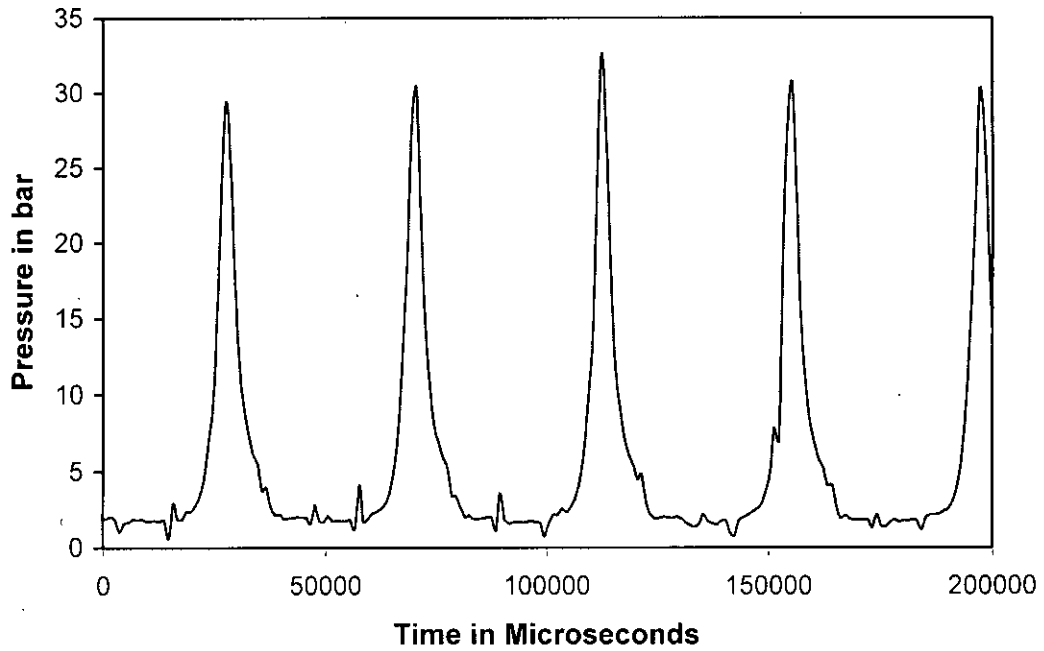


Figure-4.5 : Cyclic variations of P-V diagrams, 2800 rpm and 27 hp.

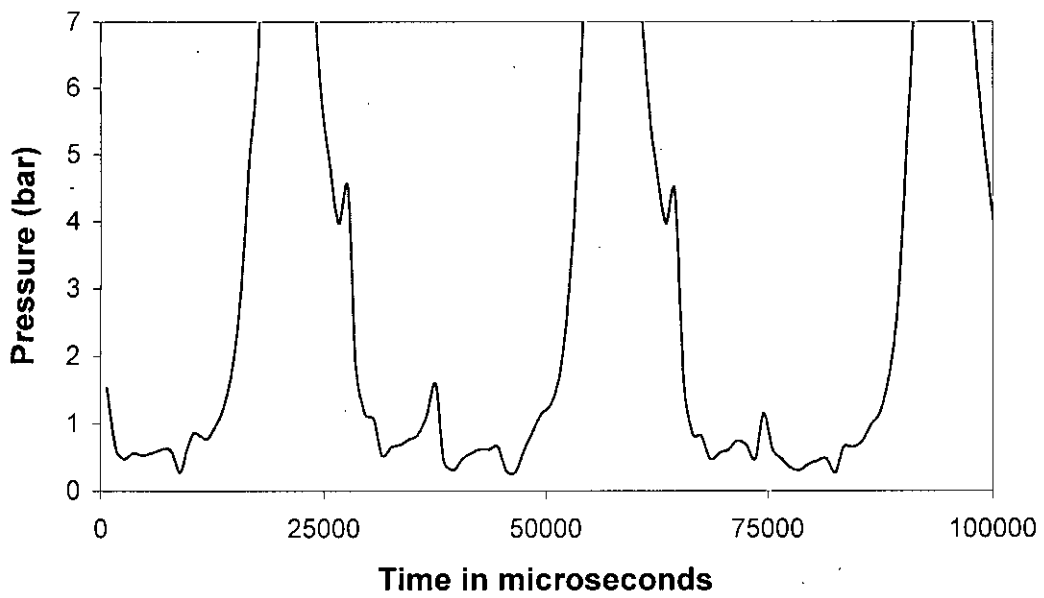


Figure-4.6 : Pressure variation during suction and exhaust strokes, 3200 rpm.

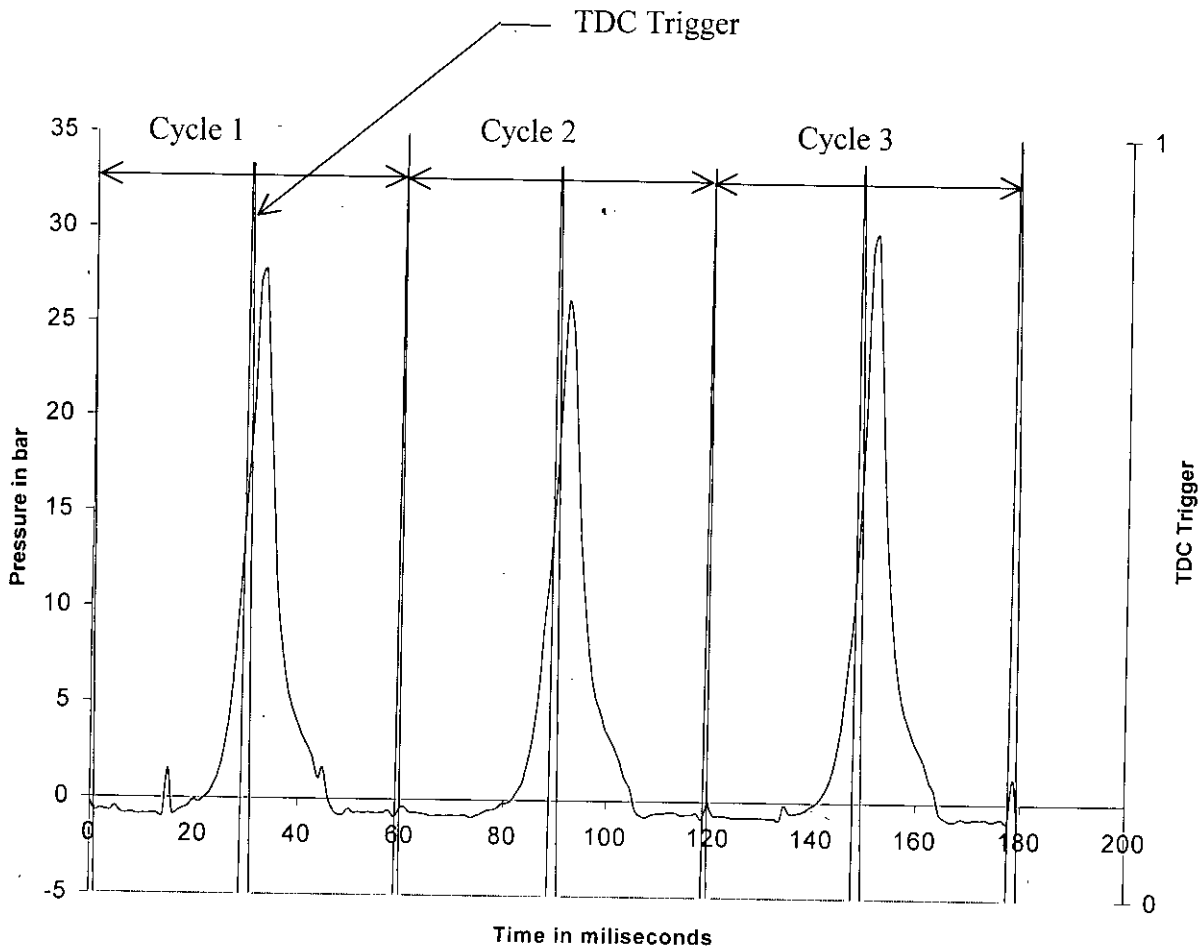


Figure 4.7 : P-t diagram with TDC Trigger at 2000 rpm and 19 hp.

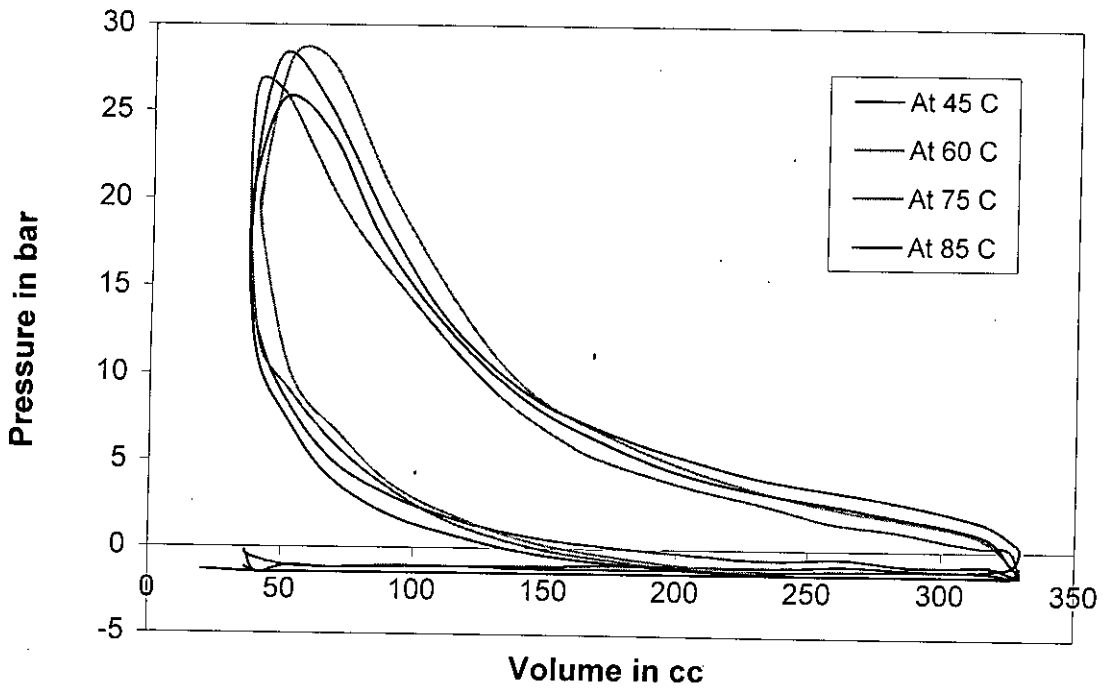
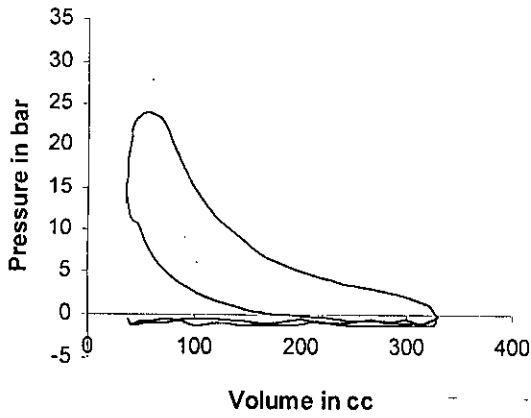
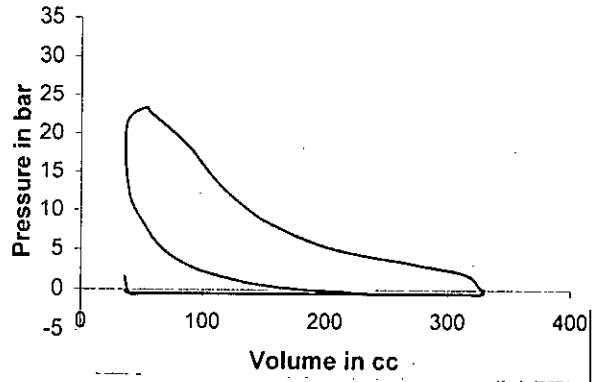


Figure-4.8 : P-V diagrams at different coolant temperatures, 2000 rpm and 19 hp.

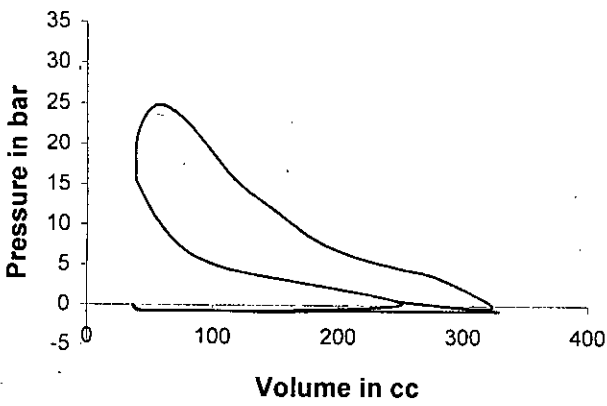
P-V Diagram at 1600 rpm and 26 kg load



P-V Diagram at 2000 rpm and 28 kg load



P-V Diagram at 2400 rpm and 29 kg load



P-V Diagram at 3200 rpm and 26 kg load

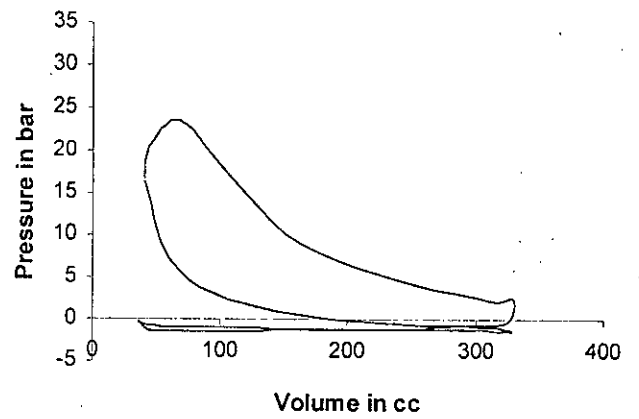


Figure-4.9 : P-V diagrams at different load conditions, 60°C.

4.4 Temperature Variations

As stated before the power output level did not vary much with the variation of coolant temperature, but it had significant effect of the Lubricating oil and engine body temperature. This temperature rise is evident in figure-4.10 and figure-4.11. Effect on exhaust gas temperature was minimum as shown in figure-4.12, which indicates that variation of coolant temperature has not effected the combustion process significantly.

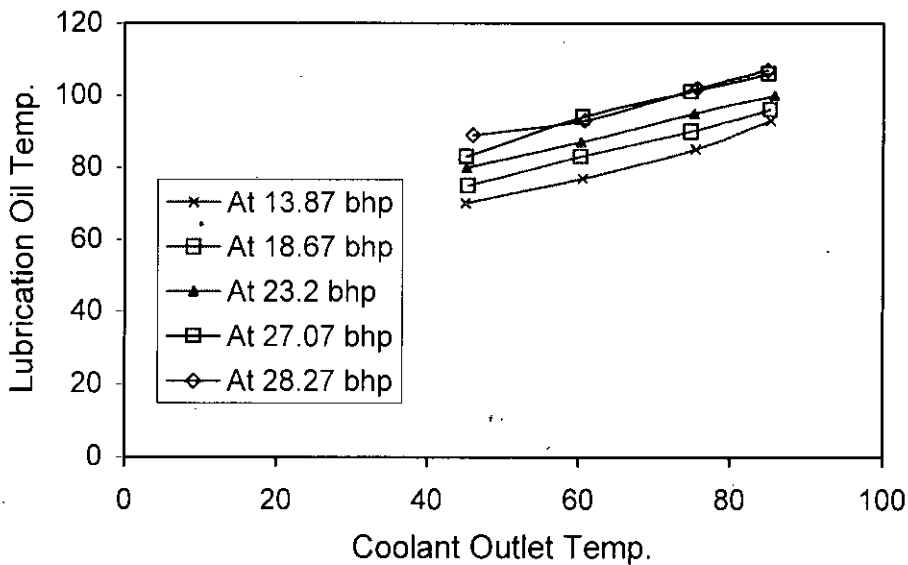


Figure-4.10 : Variation of Lubricating oil temperature with coolant temperature.

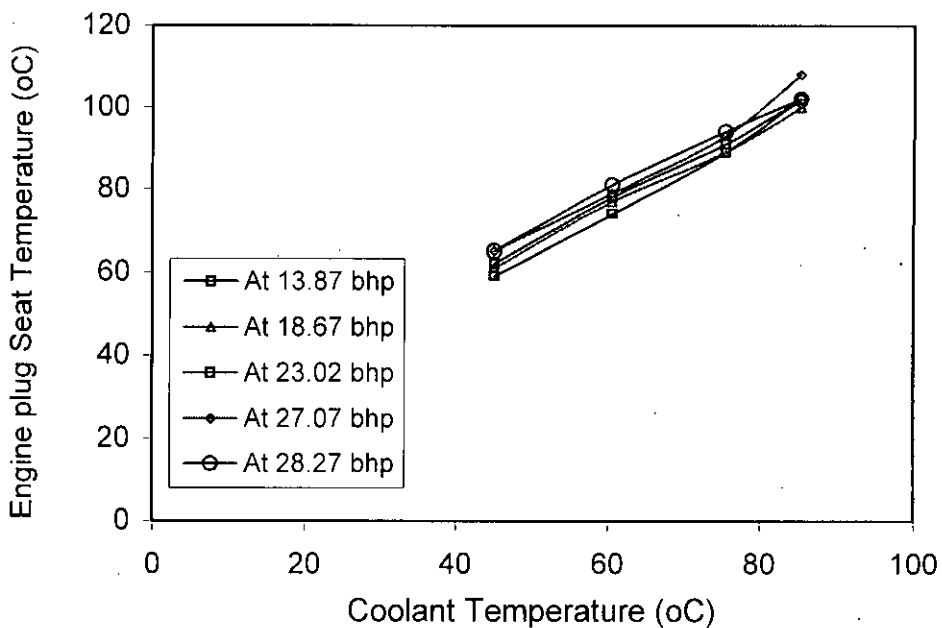


Figure-4.11 : Variation of engine body temperature with coolant temperature.

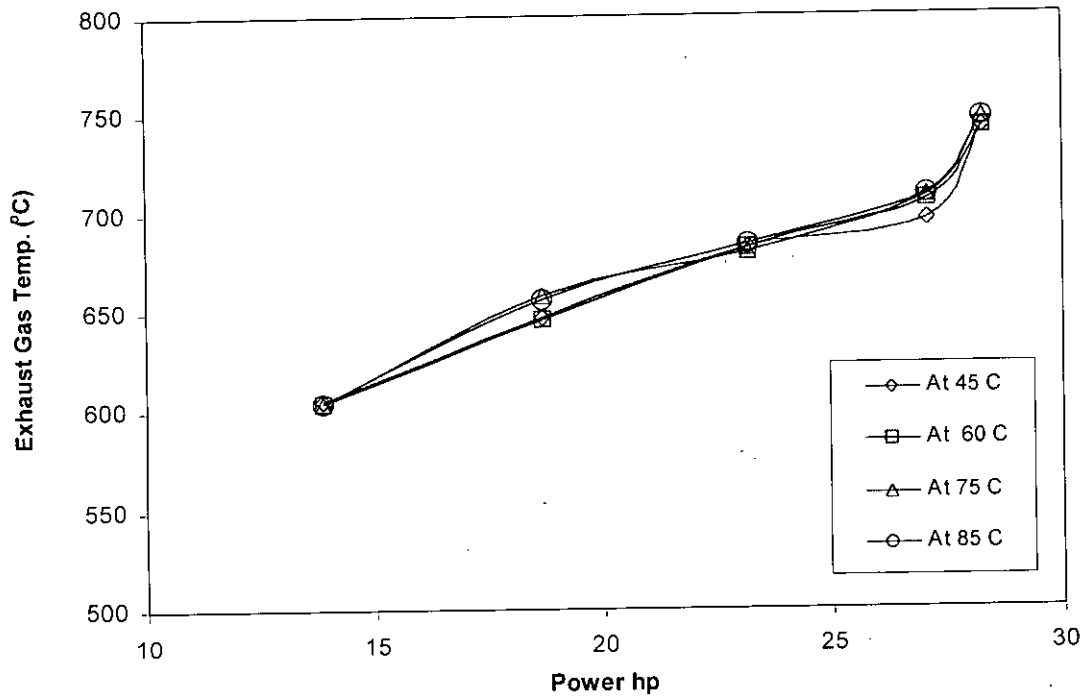


Figure-4.12 : Variation of exhaust gas temperature at different coolant temperature.

4.5 Variations in Emission

Little effect was observed in the exhaust emission analysis, as the coolant temperature was varied. The small variations in CO and CO₂ levels are more due to variation of sampling rather than real change in trends. Figure-4.13 shows the variation in emission characteristics.

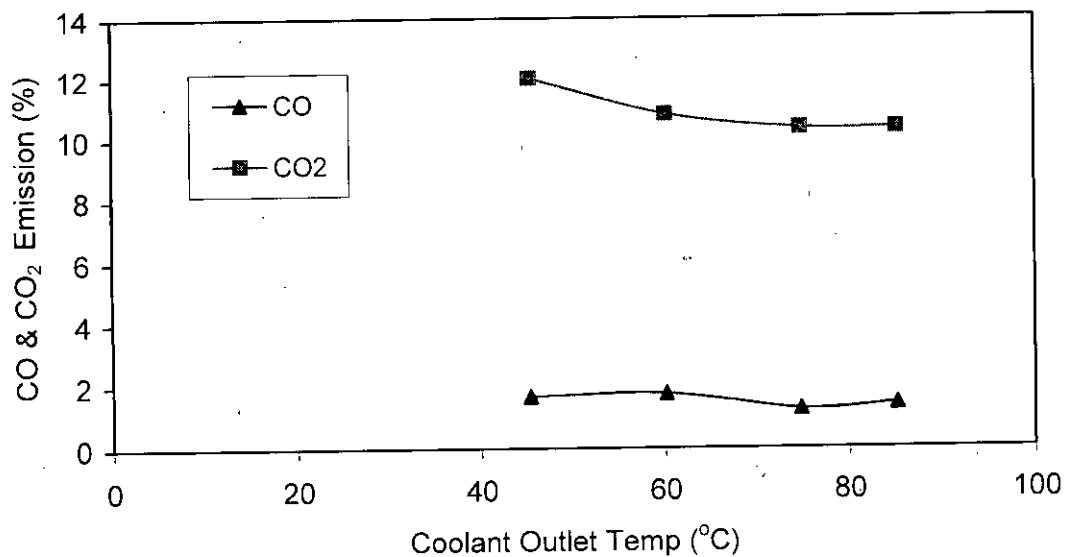


Figure-4.13 : Variation of CO and CO₂ emission with coolant temp, (2000 rpm, 18 hp).

CHAPTER 5

CONCLUSIONS AND RECOMMENDATIONS

CONCLUSIONS AND RECOMMENDATIONS

5.1 Conclusions :

The main conclusions from this experimental investigation can be summarized as the following:

- The change of water outlet temperatures in the range of 60-85°C did not show significant change on the indicator diagram (P-V) and pressure-time (P-T) variation produced inside the engine cylinder. But the high speed data acquisition of the pressure variation revealed some interesting intricate details of the cyclic variations of these parameters. The peak pressure levels were found to vary within about $\pm 10\%$ at any power level and this did not vary much with the variation of the engine speed and power level. Pressure fluctuations evident at the low pressure-levels were the result of the opening and closing of intake and exhaust valves [Heywood 1988].
- The change of water outlet temperatures in the range of 60-85°C did not show significant change on the power produced by the engine but some improvement was evident on the brake specific fuel consumption rate. With the power varying from 13.8 hp (10.2 kW) at 1600 rpm to 27.7 hp (20.4 kW) at 3200 rpm, the brake specific fuel consumption rate was found to decrease from about 257 g/hp-h to about 218 g/hp-h. At each power level the increase of the cooling temperature was found to have some effect on the brake specific fuel consumption rate, which was improved by 1-2%. Elevated water temperature must have reduced the heat losses to cooling water which is conducted through the cylinder walls. As a result this produces some improvement in fuel consumption rate. The effect on the combustion process or flame temperature was less significant evidenced by much smaller change in combustion temperature. The small reduction in fuel flow rate increased the air-fuel ratio to some extent.

- The variations of peak pressure level did not result in significant change in the output power. Two reasons are mostly responsible for such tolerance. Firstly - although the peak pressure level changes more than 10%, this acts only for a small fraction of the total cycle time accompanied by very small change in volume as the piston is in the vicinity of the top dead center, resulting in relatively small change in the work done. Secondly - phased over lapping of the four cylinder cycles and the presence of flywheel further smoothens out the final power output, resulting in smooth engine operation.
- Some variation in the lowest pressure level was observed as the engine speed increased. Varying speed from 1600 rpm to 3200 rpm this lowered the suction pressure in the order of 0.3 bar. Although this increases the pumping work during suction this again does not have significant effect on the net work done and hence the power output of the cycle, due to the very small amplitude of pressure variation.
- The corners of the pressure-volume diagram were found to be rounded [Heywood 1988] as expected which is different from the ideal Otto cycle. This is resulted from the overlapping of the valve timings and because the opening and closing of real valves are not instantaneous and take some time.
- The coolant water outlet temperature was varied through 45-85°C by adjusting the water flow. So heat losses to the cooling water was rather controlled qualitatively (lower mass flow and higher temperature difference), rather than quantity. On the other hand the elevated water temperature in the water-jacket could have quantitatively influence the combustion process and heat losses to some extent. Increasing the coolant outlet temperature was limited to 85°C because above this temperature the lubricating oil and engine body temperatures were not stabilizing, making the engine too over heated. Local boiling around the cylinder jacket most probably starts creating vapor locks which restrict further heat transfer to water. This was also evident with the passage of vapor bubbles visible through the transparent coolant flow meter.

- The variation in coolant temperature was found to have significant effect on the lubricating oil temperature and the temperature of the engine body. The effect on the exhaust gas temperatures was relatively much less significant. The exhaust gas temperature varied from 604°C to 745°C within the power range tested. For each power level the variation was less than 10°C with the change of the coolant outlet temperature. So it can be argued that the elevation of the water temperature outside the cylinder has not significantly changed the combustion process.
- The lubricating oil temperatures varied in a band of 70-93°C at 1600 rpm to 89-107°C at 3200 rpm. The average lubricating oil temperature was found to rise about 20°C for a water temperature rise of 40°C. This is within the working range of the multi grade viscosity oil used (BP, SAE20W50)[Marks' Standard Handbook 1996, Crouse et. al. 1998]. So significant change of viscosity and hence frictional losses were not evident. The situation might have more detrimental effect if lubricating oil of single grade is used.
- Rising water temperature has significant effect on the temperature of the engine body parts. Variation of a spark plug seat temperature was recorded. At 45°C water outlet temperature the engine body temperature varied from 59-65°C in the power range. This was elevated to about 102-108°C for a water temperature of 85°C. Definitely for the inner parts of the engine the rise in temperature is much more. This may have detrimental effect on the operating life of different metallic and non-metallic engine parts. Probably the effect on engine parts which withstand the highest temperatures (eg, combustion chamber, exhaust valves etc.) will be less significant as the exhaust temperatures do not change significantly.
- The exhaust emission characteristics support the argument of little change in combustion characteristics. There was some variation in CO formation accompanied by small change in CO₂ produced during combustion, as the

water temperature was elevated. The remaining O₂ and unburned HC was found to vary correspondingly within a small band. These small variations are more to do with the sampling of gases rather than showing real trend of change. Generally speaking the emission characteristics did not change significantly with the temperature of the coolant water.

- The inclusion of the effect of spark timing into the present study could be an important investigation. The spark advance is changed automatically by the ignition system with varying engine speed and load conditions. A signal recorded to identify the exact timing of the spark may reveal more interesting details regarding the cyclic pressure variation.
- Taking temperatures at more engine locations, specially inside the cylinder head with sufficiently high frequency response could identify the nature of variation of the combustion temperature as the coolant temperature changes.

5.2 Recommendations :

For future work in this field the author would like to make the following recommendations :

- More extensive experimental work, considering different variables could be performed.
- Inclusion of NO_x in the exhaust emission analysis would be useful.
- Similar studies can be carried out using other fuels, specially gaseous ones, like - compressed natural gas (CNG), bio-gas (constituting more than 60% methane) and liquefied petroleum gas (LPG).

REFERENCES

Adler Eds U. et.al. : *Automotive Handbook*, Robert Bosch GmbH, Stuttgart, 1993.

A.V. Kulkarni : *New Generation small block V8 Engine*, Technical report, Society of Automotive Engineers, 1992, SAE 920673.

Cheng, W. K., Hamrin, D., Heywood, J. B., Hochgreb, S., Min, K. and Morris, M. : *An Overview of Hydrocarbon Emissions Mechanism in Spark Ignition Engines*, Technical Report, SAE 1993, SAE 932708.

Committee on Fuel Economy of Automobiles and Light Trucks. *Automotive Fuel Economy – How Far Should We Go ?* Technical Report, Energy Engineering Board, Commission on Engineering and Technical Systems, National Research Council, 1992.

Crouse, W. H., Anglin, D. L. : *Automotive Mechanics*, Tenth Edition, McGraw-Hill Inc., 1988.

Draper C., and Li Y. : *Principles of Optimizing Control Systems and an Application to the Internal Combustion Engine*, ASME publications, 1951.

Finlay, I. C., Harris, D., Boam, D. J. and Parks, B. I. : *Factors Influencing Combustion Chamber Wall Temperature in a Liquid-Cooled, Automotive, Spark-Ignition Engine*, Proc. Instn Mech. Engrs, vol. 199, no. D3, p 207-214, 1985.

Frank, Richard M. and Heywood, John B. : *Effect of Piston Temperature on Hydrocarbon Emission from a Spark-Ignited Direct-Ignited Engine*, SAE Tran. V 100 n sect 3 1991 910558, p 820-828.

French, C. C. J., and Atkins, K. A. : *Thermal Loading of a Petrol Engine*, Proc. Instn Mech. Engrs, vol. 187, 49/73, p 561-573, 1973.

Greene, D. L. and Sanitini, D. J. : *Transportation and Global Climate Change*, American Council for an Energy Efficient Economy, Washington, D. C. and Berkeley, CA, 1993.

Heywood, J. B. : *Internal Combustion Engine Fundamentals*, McGraw Hill International editions, Automotive Technology Series, 1988.

Hucho, W. H. and Sovran, G. : *Aerodynamics of road vehicles*, Annu. Rev. Fluid Mech., 25:485-537, 1993.

Jacobson and Marcus : *Comparative Methods of Measuring Peak Pressures in Internal Combustion Engines*, Environ Eng. v 12 n 1 1999 Prof. Eng. Publ. Ltd. , p 26-28.

Kerley, R. V. and Thurston, K. W. : *The Indicated Performance of Otto-Cycle Engine*, SAE Trans., vol. 70, p 5-30, 1962.

Kim, T., Noh, S., Yu C. and Kang, I. : *Optimization of Swirl and Tumble in KMC 2.4L Lean Burn Engine.* Technical Report, SAE 1994, SAE 940307.

Klimstra, J.: *The Optimum Combustion Phasing Angle – a Convenient Engine Tuning Criterion,* SAE Paper No. 852090.

Leisenring, K., Samimy B., and Rizzoni, G. : *IC Engine Air/Fuel Ratio Feedback Control during Cold Start,* SAE Paper No. 961022.

Lumley, J. L. : *Engines An Introduction,* Cambridge University Press, 1999.

Marks' Standard Handbook for Mechanical Engineers, Tenth Edition, McGraw-Hill International Editions, Mechanical Engineering Series, 1996.

Powell, J. D. : *Closed Loop Control of Spark Advance using Cylinder,* Proceedings of the Int. Assn. Of Vehicle Design, Special Publication SP4, pp. 113-125, 1983.

Taylor, C. F. : *The Internal Combustion Engine in Theory and Practice,* Vol. 1, MIT Press, Cambridge, MA, 1966.

Tunestal P., Wilcutts M., Lee A. T. and Hedrick J. K.: *Calculation of Heat Release Energy from Engine Cylinder Pressure Data,* SAE Spec Publ v 1315, Feb 1998, Proceedings of the SAE International Congress & Exposition, Detroit, MI, p 101-112.

Wibberley, P., and Clark, C. : *An Investigation of Cylinder Pressure as Feedback for Control of Internal Combustion Engines,* SAE Paper No. 890396.

APPENDIX – A.1

PETROL ENGINE AND TEST BED

(Model: GWFS-30 / 120-L)

A1.1 Features:

GWFS-30 / 120-L Petrol Engine and Test Bed has been designed by Tokyo Meter Co. Ltd. to study and learn by experimentation in a laboratory type environment the basic fundamentals of Engine Performance Test.

- ◆ Full performance test possible
- ◆ Full engine instrumentation
- ◆ Full heat balance obtainable
- ◆ Full quantitative studies possible
- ◆ Engine and Hydraulic dynamometer completely accessible
- ◆ Components and instruments by internationally known manufactures.

A1.2 Specifications:

Test Engine, Supporting mechanism and Joining device:

Engine Model : *A12*

Engine Manufacturer : *Nissan Motor Co. Ltd., Tokyo, Japan*

Type : *water cooled, 4 cycle, gasoline engine*

Number of cylinder – bore x stroke (piston displacement)
: *4 – 73 x 70 (1171 cc)*

Compression ratio and starting device
: *9 to 1, cell motor drive*

Power at specific rpm
: *30 hp / 3200 rpm (max)*

Engine supporting mechanism
: *Channel-welded structure plate mounting system*

Joining device to dynamometer
: *Splined, double universal joint shaft*

Exhaust tube

: *Stainless flexible tube attached with connection holes for pick up of exhaust gas pressure, exhaust gas temperature and exhaust gas sample*

Accessories and fittings

: *Battery, start switch, cell motor, regulator, throttle valve & emergency stop valve, glow signal, battery charging lamp.*

Dynamometer & Joining device :

Model : *TFS – 120 L*

Form : *Hydraulic dynamometer*

Max. absorbing horse power
: *120 hp*

Max. absorbing shaft rotational speed (rpm)
: *8000 rpm*

Torque indicator : *Load cell and digital panel meter*

Tachometer : *Electro-magnetic pulse generator, digital panel meter.*

Other particulars:

Flow meter for cooling water
: *Float type area flow meter (eye view) 1000 L / H*

Fuel consumption meter
: *Skewer type 3-ball of 30, 50, 100 cc*

Throttle valve open indicator device
: *Resistance, DC generator transducer, accurate electric indicator with DC power source*

Suction air flow & pressure measuring device
: *Round accurate nozzle, dial manometer, pulsation absorbing surge tank with tension changeable diaphragm.*

APPENDIX – A.2

PRESSURE TRANSDUCER (PRESSURE PICK UP, STRAIN GAUGE PRESSURE TRANSDUCER)

A2.1 Layout

Drawing below shows an Alt. Cylinder pressure transducer (MP-50) attached directly to the engine cylinder.

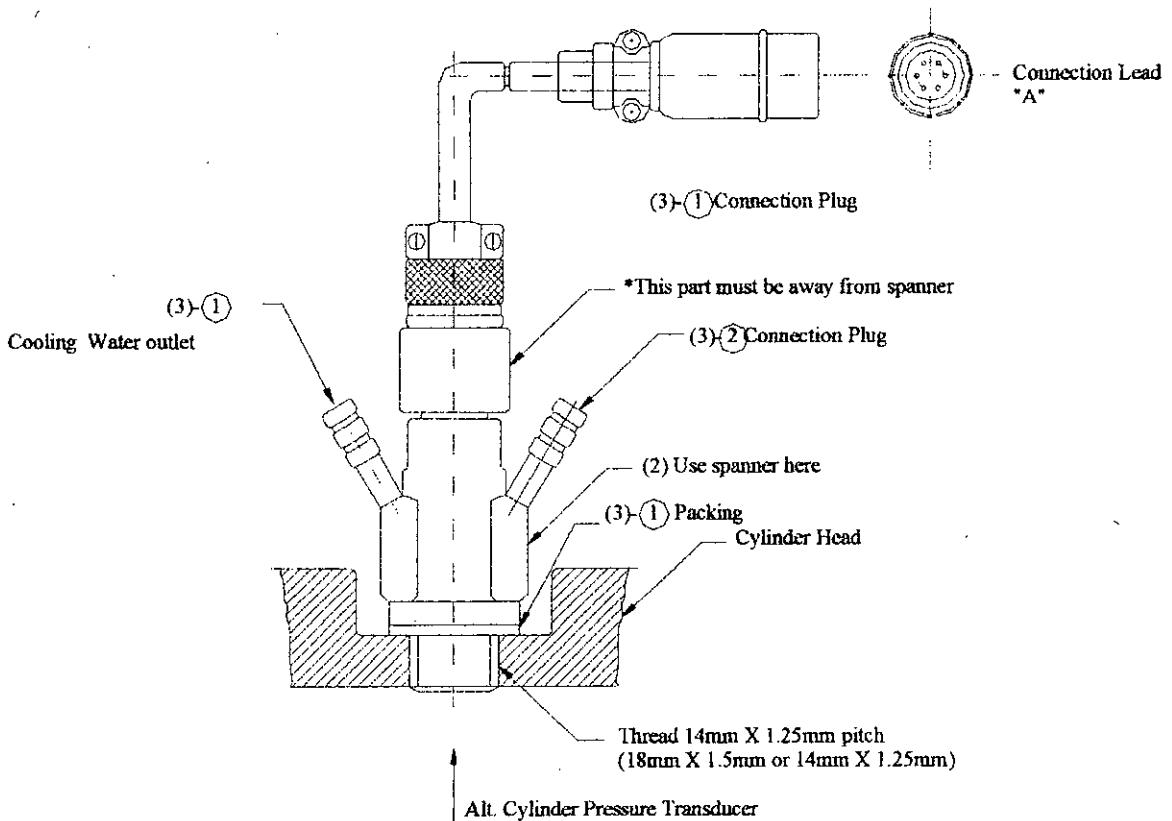


Figure-A2.1: Pressure transducer assembly for measuring in-cylinder pressure.

A2.1 Specifications:

Model	PUBME MP-50
Measuring Range	50 kg / cm ²
Form	Strain Gauge Bridge

Cooling	Water cooling
Non-linearity	Deviation : within 0.5% F.S.
Hysterisis	Deviation : within 1.5% F.S.
Natural frequency	40 kHz
Internal resistance	100 M or more

APPENDIX – A.3

CALIBRATION OF PRESSURE TRANSDUCER

A3.1 Introduction:

In order to measure the engine cylinder pressure, a pressure transducer was used. But the output from the pressure transducer was displayed as milivolts. So it was necessary to calibrate the pressure transducer to determine the relationship between its indicated voltage output and the actual pressure inside the cylinder for various piston positions.

A3.2 Equipments:

The following apparatus were used to calibrate the pressure transducer

- Dead weight pressure gauge tester
- Pressure Transducer
- Signal Conditioning Devices
- Multimeter

A3.3 Procedure:

The pressure transducer was mounted on a dead-weight pressure gauge tester with signal conditioning devices and then different pressure is applied on the tester. The corresponding voltage output was recorded in a multimeter. To verify the accuracy of the ADC-11 data acquisition hardware along with its software, the PICOSCOPE program was also used with the multimeter. The output was also verified by a conventional oscilloscope. Then a curve was plotted to determine the relationship between the output voltage of the pressure transducer and the actual pressure applied to it by the dead-weight tester.

A3.4 Data and Graph :

Pressure (psi)	Voltage (mV)	Pressure (psi)	Voltage (mV)	Pressure (psi)	Voltage (mV)
10	20	120	452	230	896
20	60	130	491	240	933
30	100	140	530	250	975
40	140	150	570	260	1011
50	183	160	619	270	1055
60	225	170	658	280	1094
70	266	180	701	290	1128
80	308	190	737	300	1171
90	247	200	775	310	1210
100	396	210	817		
110	416	220	855		

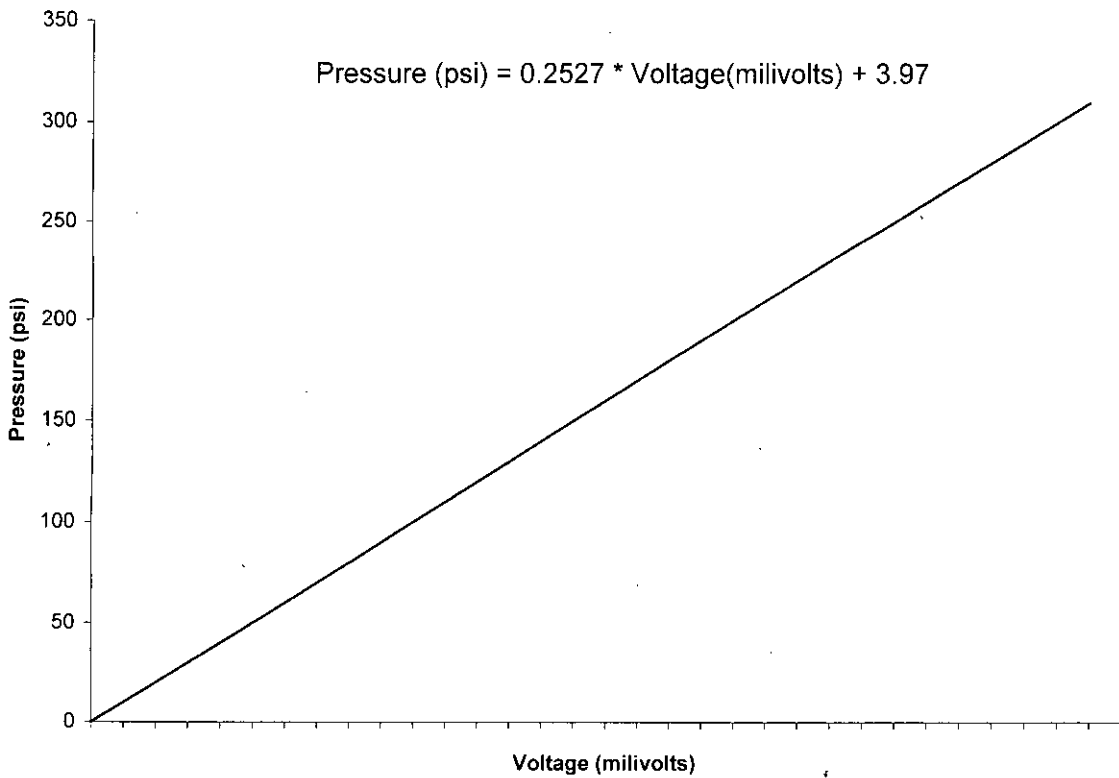


Figure A3.1: Pressure vs. voltage diagram for the pressure transducer.

A3.5 Pressure-Voltage Relation:

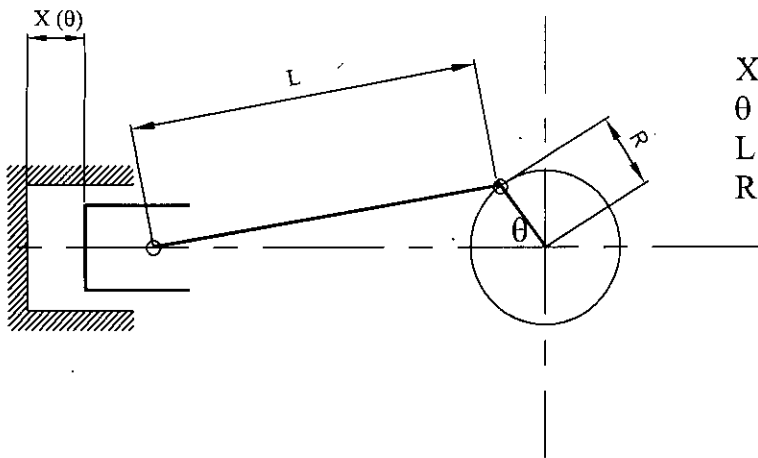
From the pressure vs. voltage diagram we get the following relationship between the pressure applied to the pressure transducer and the corresponding output voltage shown by it.

$$\text{Pressure (bar)} = 0.0172 * \text{Voltage (milivolts)} + 0.27$$

A3.6 Generation of P-V diagram:

The output from the pressure transducer as well as the TDC Detector were simultaneously logged by the data acquisition hardware. From the TDC trigger data, the total time in-between three successive TDC position was taken as one cycle time and the instantaneous crank angle (Taking TDC position as 0°) during that cycle is then calculated using a linear relationship between Total cycle time and Total crank angle (720°). Piston distance factor (from TDC) X as a function of crank angle is calculated using a standard formula as given below (for this engine, L/R=8):

$$X(\theta) = (1 - \cos \theta) \left[1 + \frac{1}{1 - \cos \theta} \left\{ \left(\frac{L}{R} \right) - \sqrt{\left(\frac{L}{R} \right)^2 - \sin^2 \theta} \right\} \right]$$



- X (θ) : piston distance from TDC
- θ : crank angle
- L : connecting rod length
- R : crank radius

Finally, by multiplying the total swept volume (292.97cc) of the cylinder with X/2, we get the value of instantaneous swept volume for all piston positions.

APPENDIX – A.4

ADC-11

A4.1: Introduction

ADC-11 provides 11 channels of analog input in a case slightly larger than a matchbox. A digital output is provided for control / alarm functions. In addition, this output can also be used to power sensors such as thermistors.

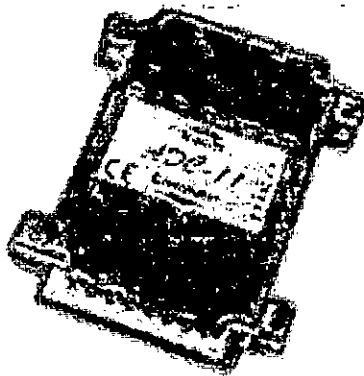


Figure A4.1: Photograph of ADC-11

A4.2 Features

- Large number of channels
- Compact design
- Digital output for control purposes
- Data logging software included
- ADC-11 terminal board provides screw terminals to simplify connection to the converter inputs.
- ADC-11 is a medium speed analog to digital converter with eleven input channels and digital output. It can be used as an oscilloscope with the PICOSCOPE program, or as a data logger using PICOLOG program.

A4.3 Specifications:

Resolution	: <i>10 bits</i>
Input	: <i>0 – 2.5 volts</i>
Input impedance	: <i>>1 ohms</i>
Number of input channels	: <i>11</i>
Maximum sampling rate	: <i>15,000 samples per second</i>
Over voltage protection	: <i>+/- 30 volts</i>
Input connectors	: <i>25 way female D-type</i>
Output connectors	: <i>25 way male D-type to computer parallel port</i>
Digital output voltage	: <i>3 – 5 volts</i>
Digital output impedance	: <i>1 – 2 ohms</i>

A4.4 Connections:

Pin	Function
1	Digital output / voltage input
2	Signal Ground
3	Analog input channel 1
4	Analog input channel 2
5	Analog input channel 3
6	Analog input channel 4
7	Analog input channel 5
8	Analog input channel 6
9	Analog input channel 7
10	Analog input channel 8

11	Analog input channel 9
12	Analog input channel 10
13	Analog input channel 11
14 – 25	Unused

Pin 1 can be used either as a digital output or as a voltage source. ADC-11 does not provide any additional protection for this output.

A4.5 Safety warning:

For all PICO ADCs, the ground input is connected to the ground of the computer. This is done in order to minimize interference. As with most oscilloscopes, it should be taken care not to connect the ground input of the ADC to anything, which may be at some voltage other than ground. Doing so may cause damage to the ADC.

APPENDIX - B

Experimental Data

Date: 25-Jun-01
 Speed : 1600 rpm
 Dry Bulb Temp : 30 °C
 Atm. Pressure : 756 mm of Hg
 Saturation Pressure of Water at Test Condition : 31.83 mm Hg
 Density of Water Vapor at Partial Pressure : 0.0304 kg / m³
 Density of Air at Test Condition : 1.14424 kg / m³
 Av. Load : 26 kg
 Wet Bulb Temp : 27 °C
 Sp. Gr. of Fuel : 0.738
 bhp (lab) 13.87
 Relative Humidity : 0.79

Coolant Outlet Temp (°C)	Coolant Inlet Temp (°C)	Suction Air Temp (°C)	Exhaust Gas Temp (°C)	Lub. Oil Temp. (°C)	Ignition Plug Seat Temp (°C)	Lub. Oil Pressure (kg/cm ²)	Dial Mano meter Reading (mm Aqua)	% of Throttle Opening	Fuel (50 cc) consumption Time (sec)	Water Flowrate (l/h)	Bsfc (gm / bhp.hr)
45	30.1	32.5	605	70	59	3	6	22	37.1	770	258.2
60.5	29.8	33	604	77	74	3	6	22	37.1	350	258.2
75.4	29.4	33.2	604	85	89	3.5	5.9	20	37.2	210	257.5
85.3	30.1	33.8	604	93	102	3.5	5.5	20	39.1	130	255.1

Coolant Outlet Temp (°C)	Air Intake Flowrate (kg/s)	Fuel Flow rate (l/h)	AFR (Calculated)	AFR (Measured)	CO (% vol.)	CO ₂ (% vol.)	HC (ppm)	O ₂ (% vol.)
45	0.013	4.85	13.28	13.8	2.45	10.57	220	0.83
60.5	0.013	4.85	13.28	13.6	3.08	10.47	270	0.83
75.4	0.013	4.84	13.21	13.6	3.12	10.5	270	0.77
85.3	0.013	4.60	13.40	13.6	3.2	10.01	190	0.81

Experimental Data

Date: 10-Jul-01
 Speed : 2000 rpm
 Dry Bulb Temp : 30.75 °C
 Atm. Pressure : 755 mm of Hg
 Saturation Pressure of Water at Test Condition : 33.2325 mm Hg
 Density of Water Vapor at Partial Pressure : 0.03165 kg / m³
 Density of Air at Test Condition : 1.14009 kg / m³

Av. Load : 28 kg
 Wet Bulb Temp : 27 °C
 Sp. Gr. of Fuel : 0.732

bhp (lab) 18.67
 Relative Humidity : 0.75

Coolant Outlet Temp (°C)	Coolant Inlet Temp (°C)	Suction Air Temp (°C)	Exhaust Gas Temp (°C)	Lub. Oil Temp. (°C)	Ignition Plug Seat Temp (°C)	Lub. Oil Pressure (kg/cm ²)	Dial Mano meter Reading (mm Aqua)	% of Throttle Opening	Fuel (50 cc) consumption Time (sec)	Water Flowrate (l/h)	Bsfc (gm / bhp.hr)
45.4	29.7	32.6	647	75	61	3.5	10	32	30.5	850	231.4
60.2	29.6	33.6	646	83	77	3.5	10	31	31	410	227.7
74.8	29.6	34	658	90	89	4	10	31	31	260	227.7
85.2	29.4	34.3	656	96	100	4	10	30	31.2	210	226.2

Coolant Outlet Temp (°C)	Air Intake Flowrate (kg/s)	Fuel Flow rate (l/h)	AFR (Calculated)	AFR (Measured)	CO (% vol.)	CO ₂ (% vol.)	HC (ppm)	O ₂ (% vol.)
45.4	0.017	5.90	14.19	14.4	1.66	12.03	215	0.87
60.2	0.017	5.81	14.42	14.5	1.75	10.83	105	0.96
74.8	0.017	5.81	14.42	14.8	1.24	10.37	90	1.03
85.2	0.017	5.77	14.51	14.7	1.41	10.37	80	1.08

Experimental Data

Date: 5-Jul-01

Speed : 2400 rpm

Dry Bulb Temp : 30.5 C

Atm. Pressure : 752 mm of Hg

Saturation Pressure of Water at Test Condition : 32.765 mm Hg

Density of Water Vapor at Partial Pressure : 0.03123 kg / m³

Density of Air at Test Condition : 1.13607 kg / m³

Av. Load : 29 kg

Wet Bulb Temp : 27.25 C

Sp. Gr. of Fuel : 0.74

bhp (lab) 23.2

Relative Humidity : 0.78

Coolant Outlet Temp (C)	Coolant Inlet Temp (C)	Suction Air Temp (C)	Exhaust Gas Temp (C)	Lub. Oil Temp. (C)	Ignition Plug Seat Temp (C)	Lub. Oil Pressure (kg/cm ²)	Dial Manometer Reading (mm Aqua)	% of Throttle Opening	Fuel (50 cc) consumption Time (sec)	Water Flowrate (l/h)	Bsfc (gm / bhp.hr)
45.2	30.7	32.4	682	80	62	3.5	16	43	25.1	970	228.7
60.3	30.4	33.7	682	87	78	3.5	15	39	25.2	430	227.8
75.2	30.6	34	680	95	91	3.5	15	39	25.1	290	228.7
85.8	30.8	34.9	684	100	102	3.75	15	39	25	210	229.7

Coolant Outlet Temp (°C)	Air Intake Flowrate (kg/s)	Fuel Flow rate (l/h)	AFR (Calculated)	AFR (Measured)	CO (% vol.)	CO ₂ (% vol.)	HC (ppm)	O ₂ (% vol.)
45.2	0.021	7.17	14.58	14.6	1.27	11.41	168	0.85
60.3	0.021	7.14	14.18	14	2.86	10.35	155	0.96
75.2	0.021	7.17	14.12	14.4	1.92	9.99	125	0.95
85.8	0.021	7.20	14.06	14.3	2.02	9.92	120	0.98

Experimental Data

Date: 29-Jun-01

Speed : 2800 rpm

Dry Bulb Temp : 30.5 °C

Atm. Pressure : 751 mm of Hg

Saturation Pressure of Water at Test Condition : 32.765 mm Hg

Density of Water Vapor at Partial Pressure : 0.03123 kg / m³

Density of Air at Test Condition : 1.135422 kg / m³

Av. Load : 29 kg

Wet Bulb Temp : 26.5 °C

Sp. Gr. of Fuel : 0.73

bhp (lab) 27.07

Relative Humidity : 0.73

Coolant Outlet Temp (°C)	Coolant Inlet Temp (°C)	Suction Air Temp (°C)	Exhaust Gas Temp (°C)	Lub. Oil Temp. (°C)	Ignition Plug Seat Temp (°C)	Lub. Oil Pressure (kg/cm ²)	Dial Mano meter Reading (mm Aqua)	% of Throttle Opening	Fuel (50 cc) consumption Time (sec)	Water Flowrate (l/h)	Bsfc (gm / bhp.hr)
45.2	30.6	33.5	696	83	65	3.5	22.5	46	21.1	910	230.1
60.5	30.3	34.6	706	94	79	3.5	23	46	21.5	510	225.8
74.8	30.1	35.1	708	101	93	3.5	22.5	46	21.5	340	225.8
85	30.5	35.4	709	106	108	3.5	22	46	21.6	130	224.8

Coolant Outlet Temp (°C)	Air Intake Flowrate (kg/s)	Fuel Flow rate (l/h)	AFR (Calculated)	AFR (Measured)	CO (% vol.)	CO ₂ (% vol.)	HC (ppm)	O ₂ (% vol.)
45.2	0.025	8.53	14.73	14.3	1.77	10.81	110	0.8
60.5	0.026	8.37	15.18	14.3	1.84	10.75	120	0.78
74.8	0.025	8.37	15.01	14.3	1.83	10.72	160	0.76
85	0.025	8.33	14.91	14.1	2.08	10.07	140	0.77

Experimental Data

Date: 16-Jul-01

Speed : 3200 rpm

Dry Bulb Temp : 30 °C

Atm. Pressure : 754 mm of Hg

Saturation Pressure of Water at Test Condition : 31.83 mm Hg

Density of Water Vapor at Partial Pressure : 0.03039 kg / m³

Density of Air at Test Condition : 1.141169 kg / m³

Av. Load : 26.5 kg

Wet Bulb Temp : 27 °C

Sp. Gr. of Fuel : 0.736

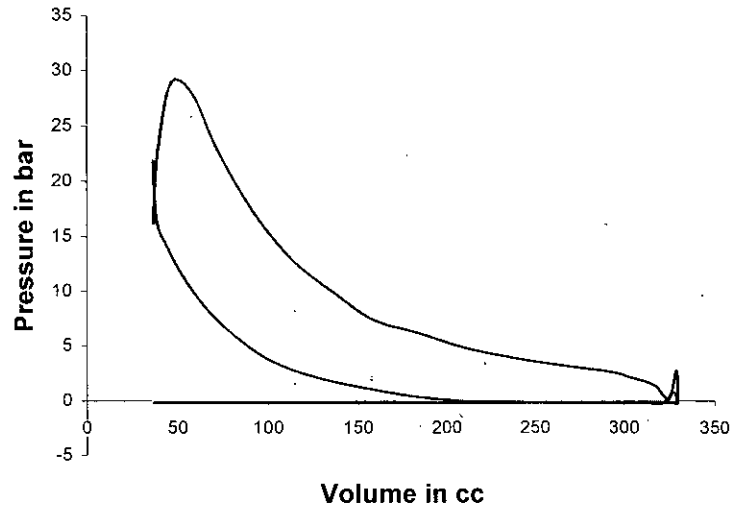
bhp (lab) 28.27

Relative Humidity : 0.79

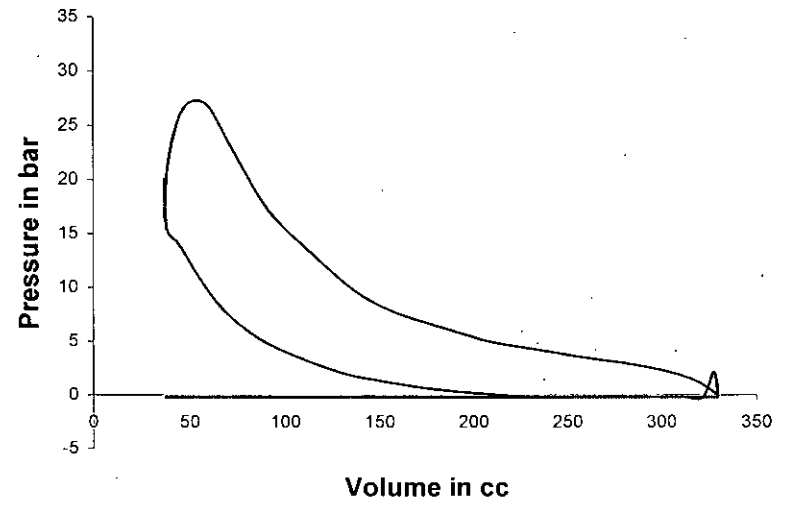
Coolant Outlet Temp (°C)	Coolant Inlet Temp (°C)	Suction Air Temp (°C)	Exhaust Gas Temp (°C)	Lub. Oil Temp. (°C)	Ignition Plug Seat Temp (°C)	Lub. Oil Pressure (kg/cm ²)	Dial Mano meter Reading	% of Throttle Opening	Fuel (50 cc) consumption Time (sec)	Water Flowrate (l/h)	Bsfc (gm / bhp.hr)
46	30.1	32.9	742	89	65	3.5	25	51	20.9	1100	224.2
60.8	29.9	34.2	742	93	81	3.5	25	51	21.1	490	222.1
75.6	29.9	34.9	747	102	94	3.5	25	51	21.5	360	218.0
84.9	29.7	35	747	107	102	3.5	25	51	21.5	270	218.0

Coolant Outlet Temp (°C)	Air Intake Flowrate (kg/s)	Fuel Flow rate (l/h)	AFR (Calculated)	AFR (Measured)	CO (% vol.)	CO ₂ (% vol.)	HC (ppm)	O ₂ (% vol.)
46	0.027	8.61	15.29	15.9	0.27	11.12	90	1.41
60.8	0.027	8.53	15.44	15.7	0.27	11.81	60	1.42
75.6	0.027	8.37	15.73	15.7	0.27	11.71	28	1.39
84.9	0.027	8.37	15.73	15.8	0.27	11.73	0	1.48

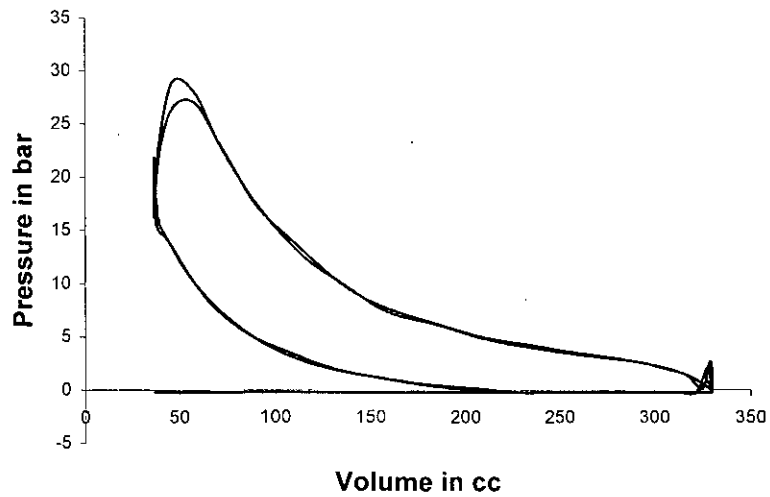
P-V Diagram at 1600 rpm and 26 kg load at 45 C



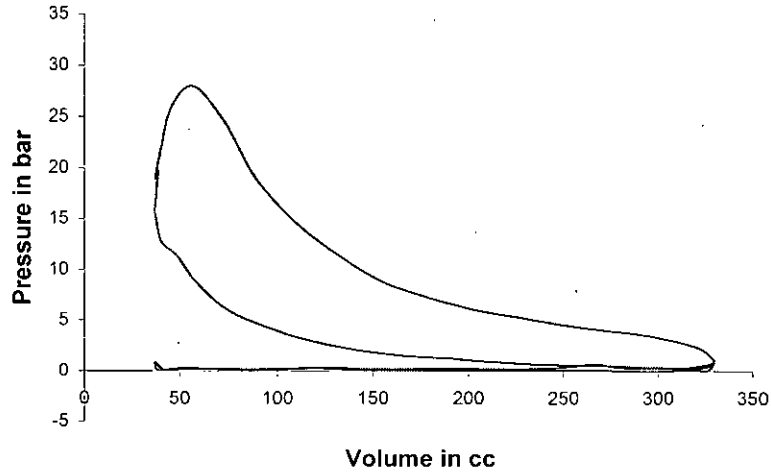
P-V Diagram at 1600 rpm and 26 kg load at 45 C



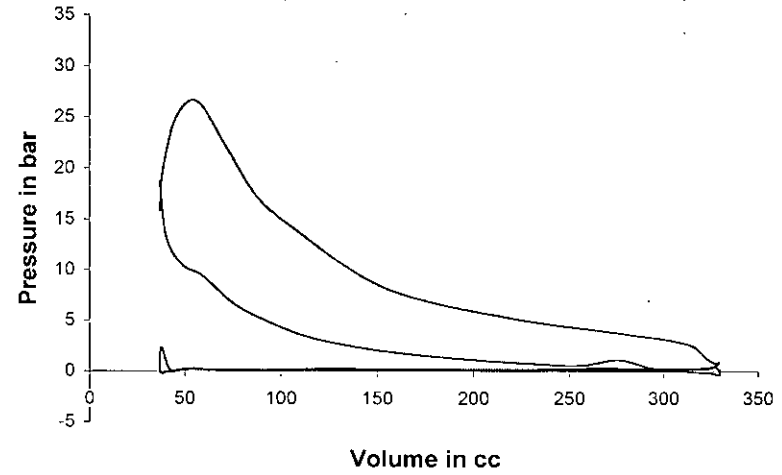
P-V Diagram at 1600 rpm and 26 kg load at 45 C



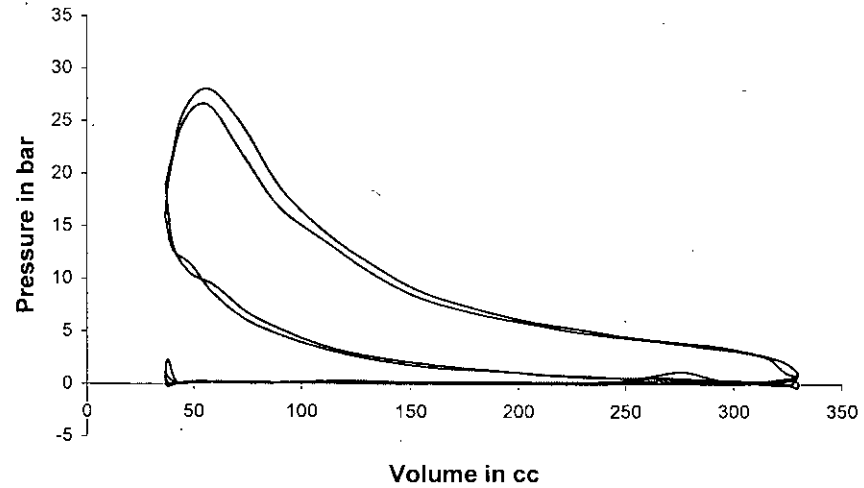
P-V Diagram at 1600 rpm and 26 kg load at 60 C



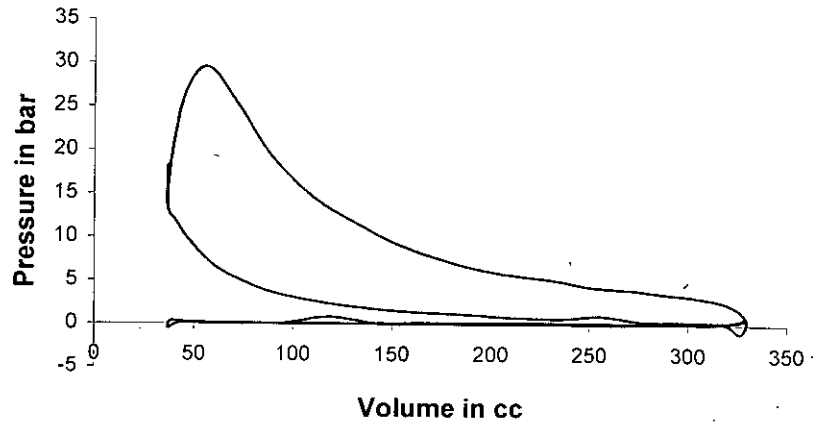
P-V Diagram at 1600 rpm and 26 kg load at 60 C



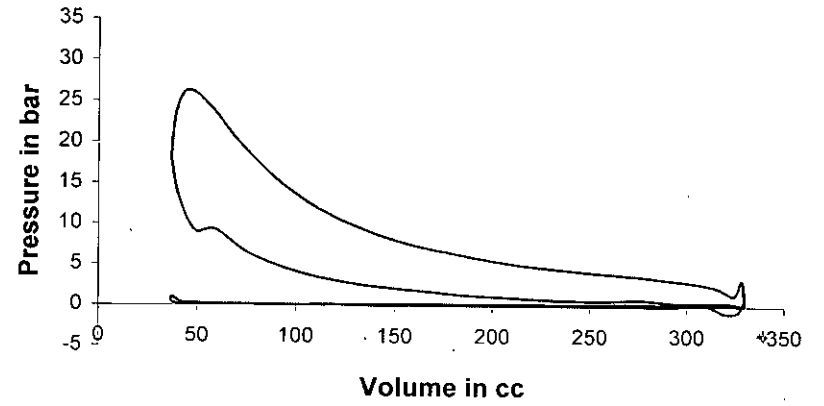
P-V Diagram at 1600 rpm and 26 kg load at 60 C



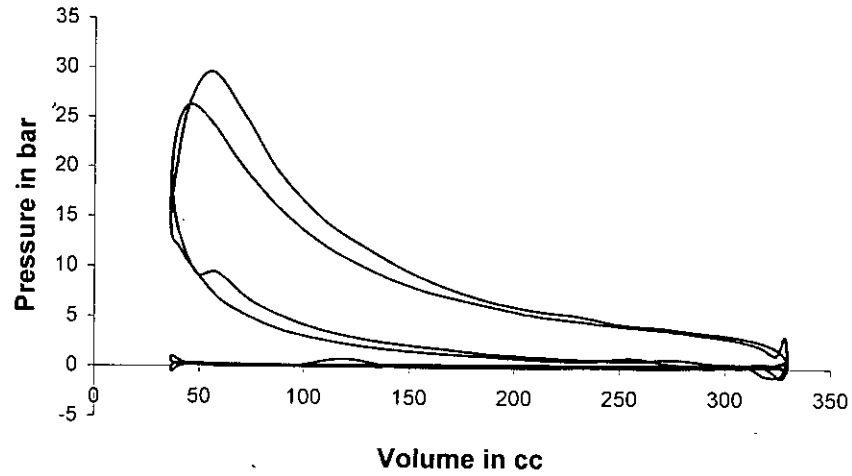
P-V Diagram at 1600 rpm and 26 kg load at 75 C



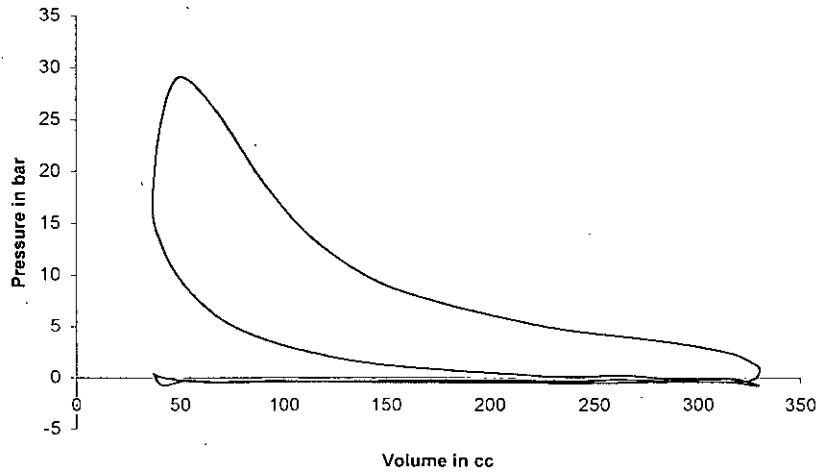
P-V Diagram at 1600 rpm and 26 kg load at 75 C



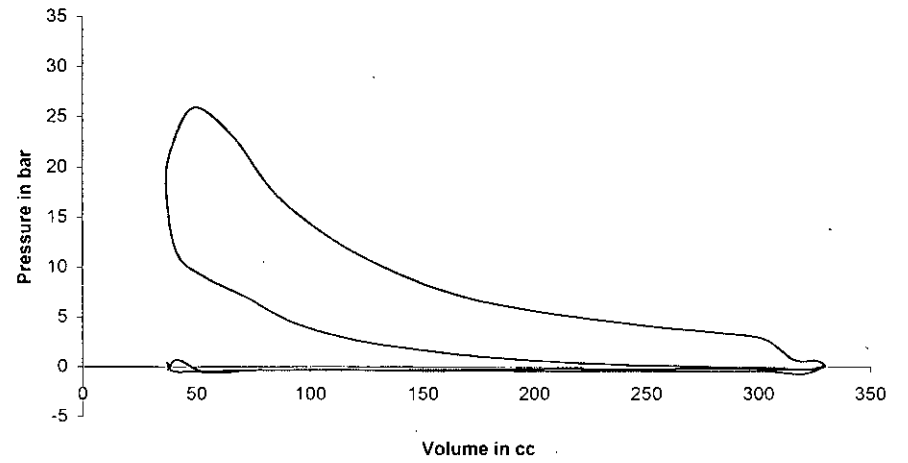
P-V Diagram at 1600 rpm and 26 kg load at 75 C



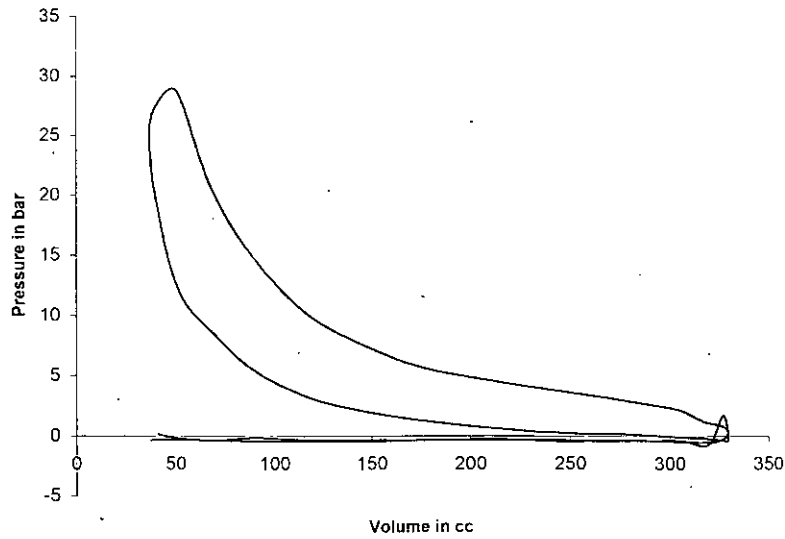
P-V Diagram at 2000 rpm and 28 kg load at 45 C



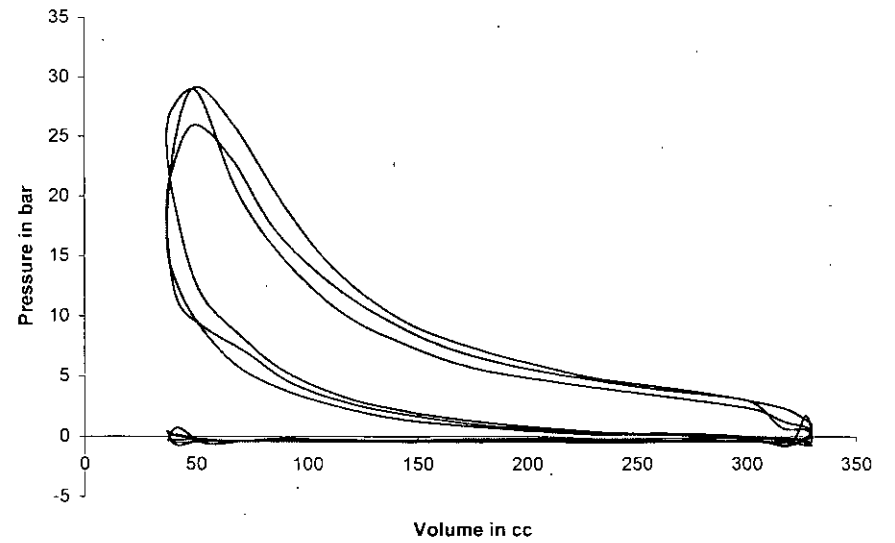
P-V Diagram at 2000 rpm and 28 kg load at 45 C



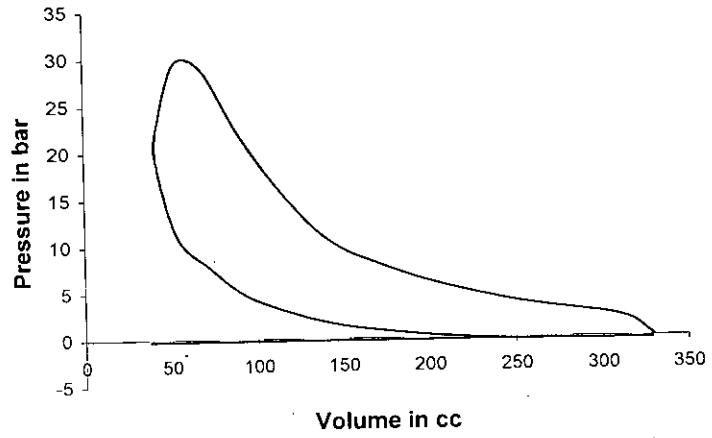
P-V Diagram at 2000 rpm and 28 kg load at 45 C



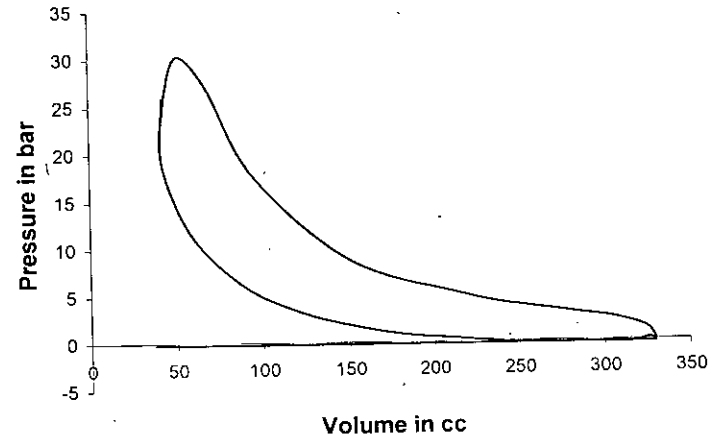
P-V Diagram at 2000 rpm and 28 kg load at 45 C



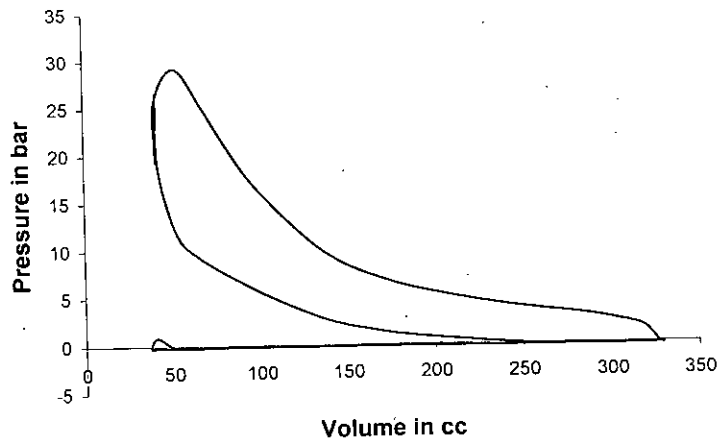
P-V Diagram at 2000 rpm and 28 kg load at 60 C



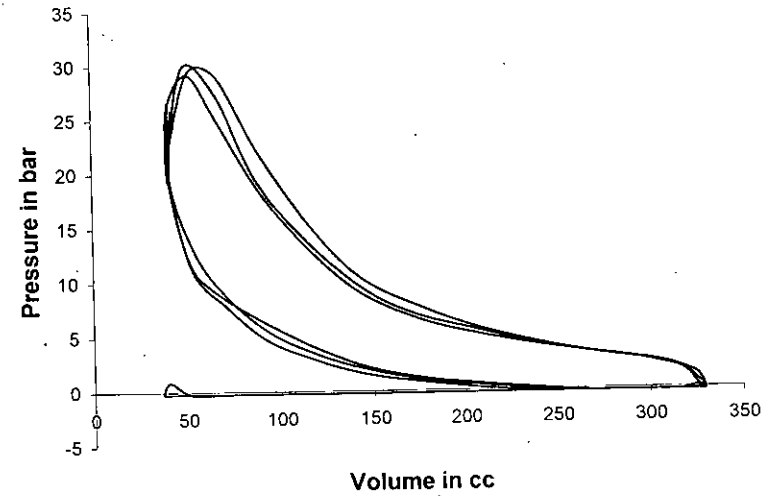
P-V Diagram at 2000 rpm and 28 kg load at 60 C



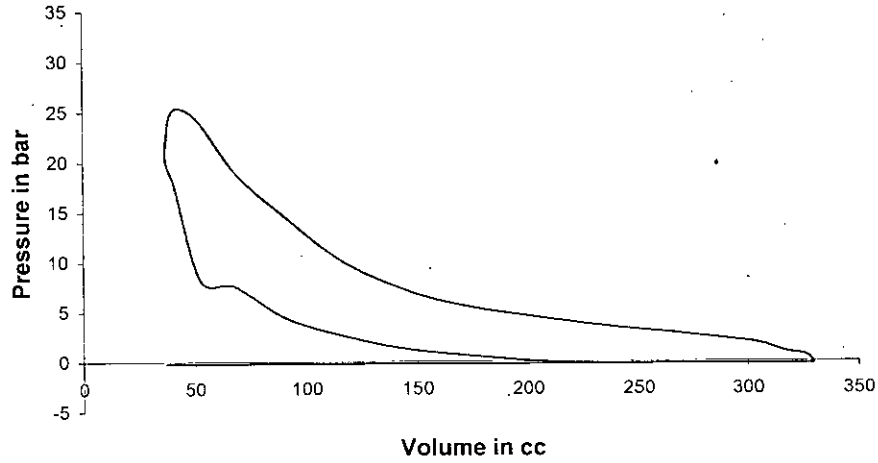
P-V Diagram at 2000 rpm and 28 kg load at 60 C



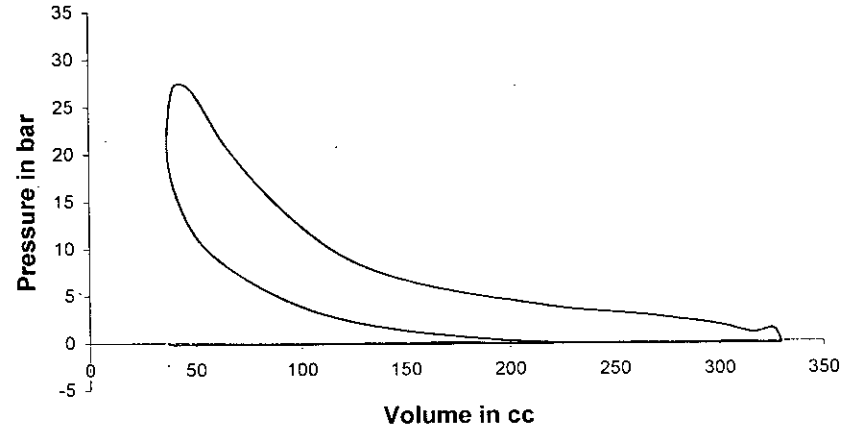
P-V Diagram at 2000 rpm and 28 kg load at 60 C



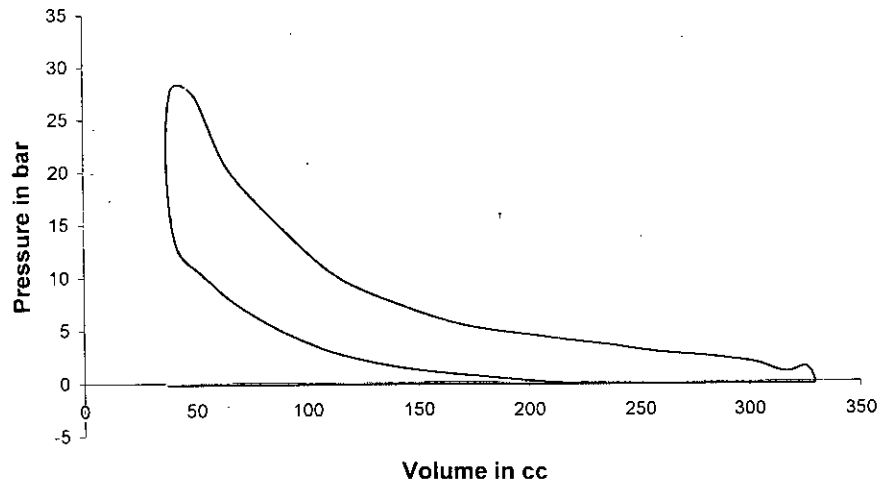
P-V Diagram at 2000 rpm and 28 kg load at 75 C



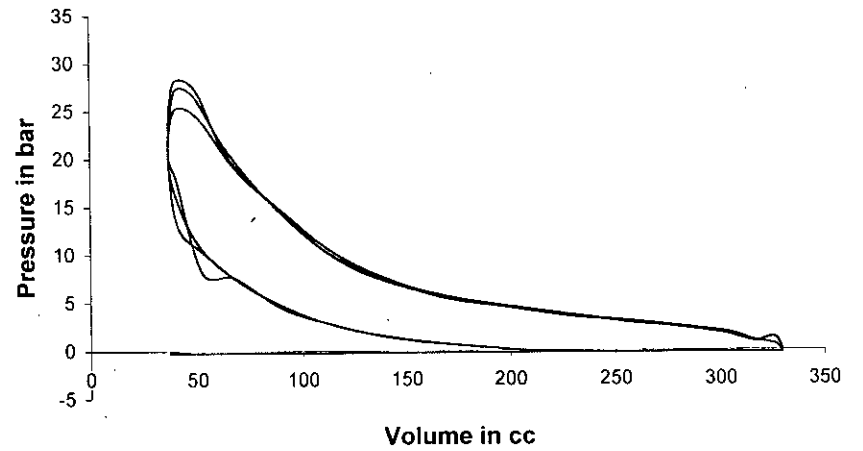
P-V Diagram at 2000 rpm and 28 kg load at 75 C



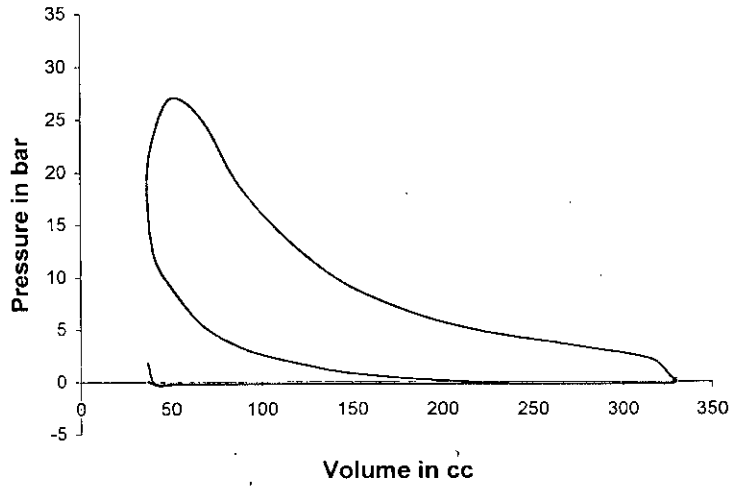
P-V Diagram at 2000 rpm and 28 kg load at 75 C



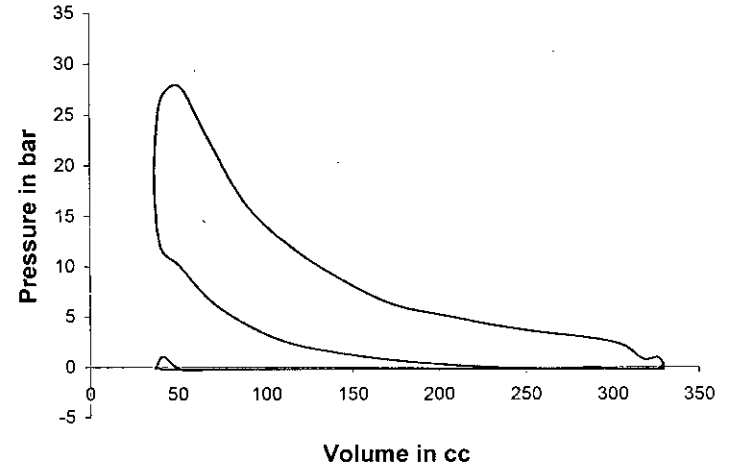
P-V Diagram at 2000 rpm and 28 kg load at 75 C



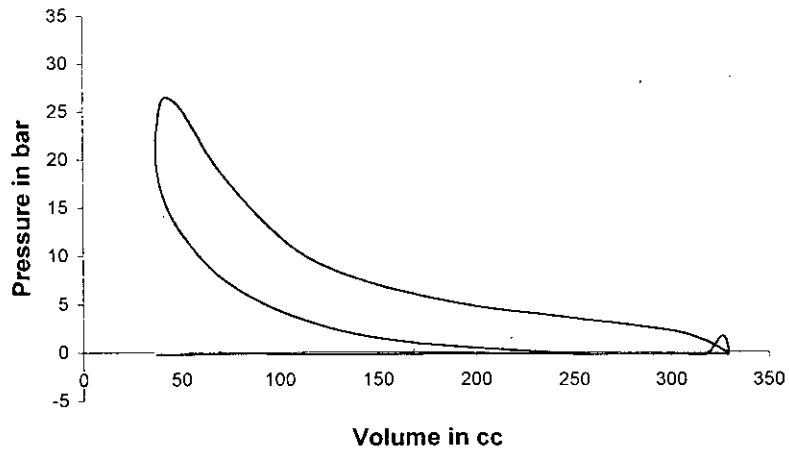
P-V Diagram at 2000 rpm and 28 kg load at 85 C



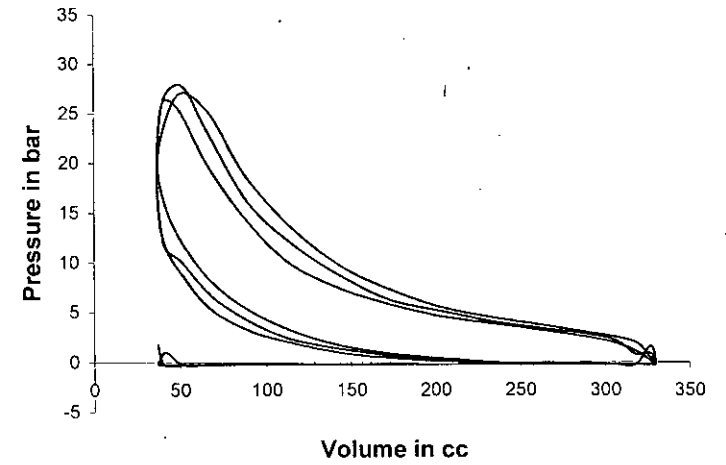
P-V Diagram at 2000 rpm and 28 kg load at 85 C



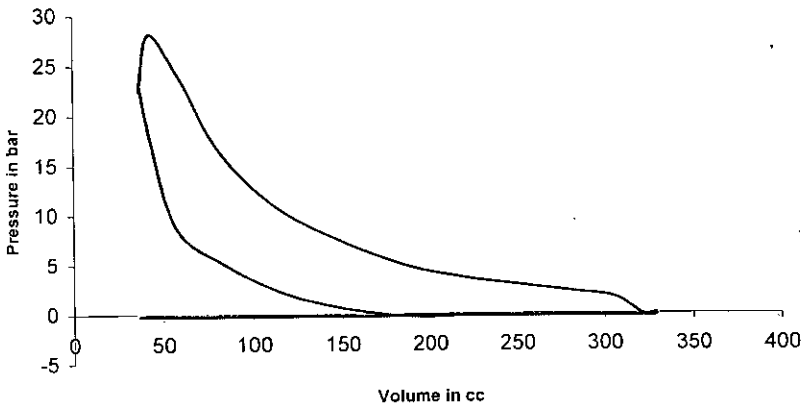
P-V Diagram at 2000 rpm and 28 kg load at 85 C



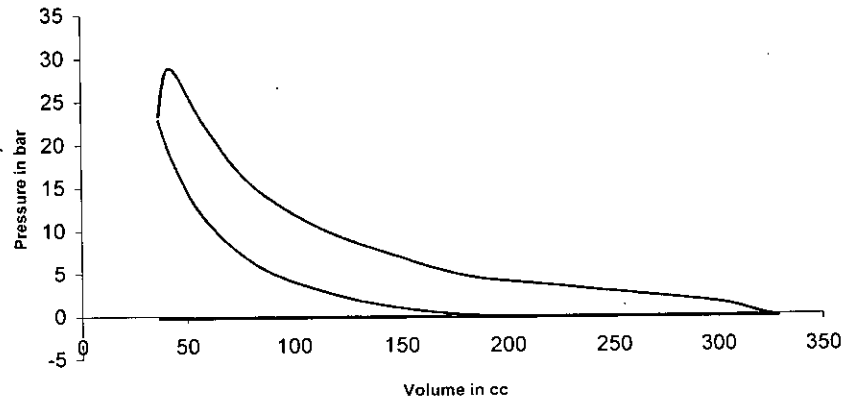
P-V Diagram at 2000 rpm and 28 kg load at 85 C



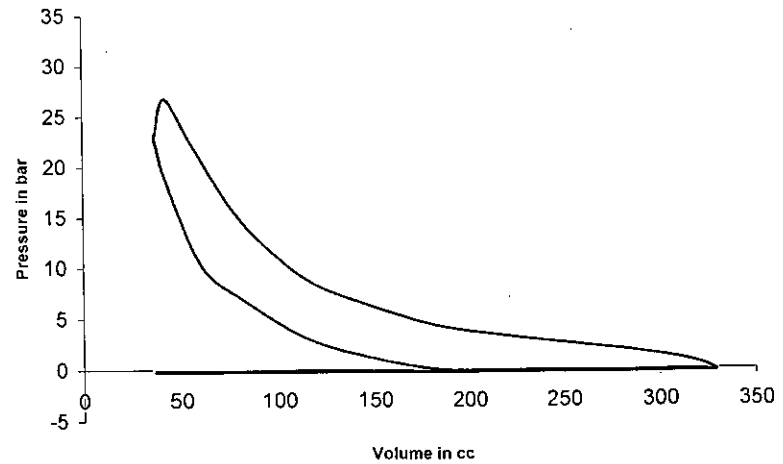
P-V Diagram at 2400 rpm and 29 kg load at 45 C



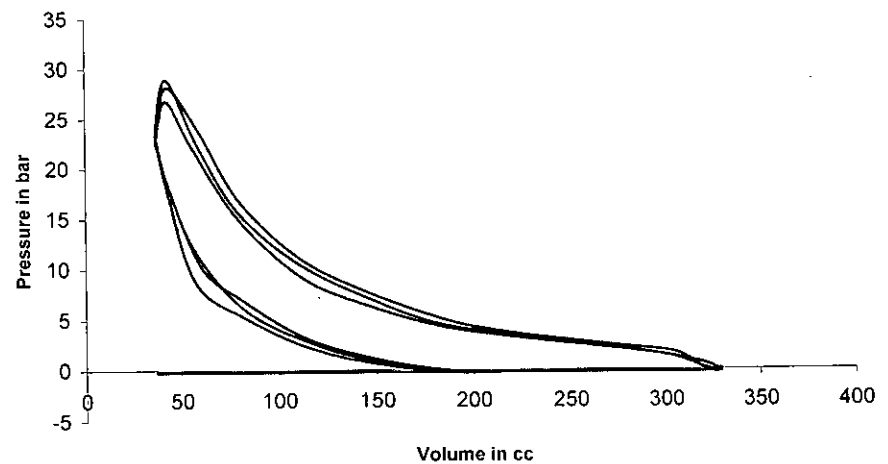
P-V Diagram at 2400 rpm and 29 kg load at 45 C



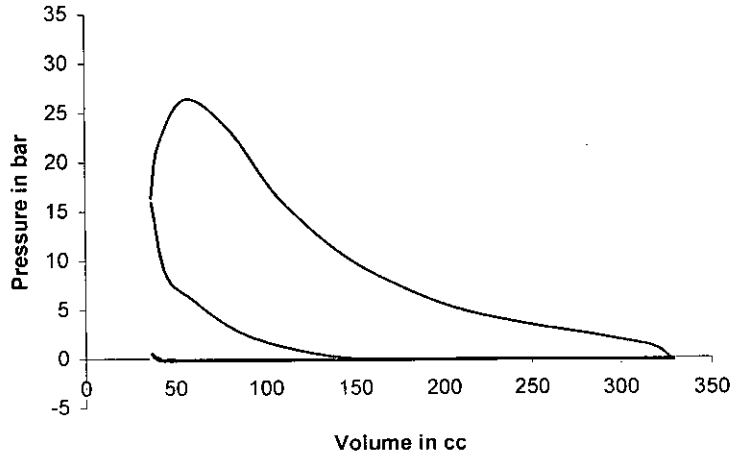
P-V Diagram at 2400 rpm and 29 kg load at 45 C



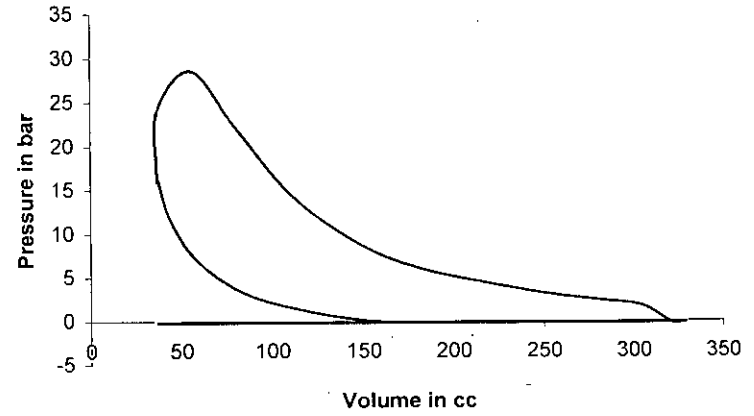
P-V Diagram at 2400 rpm and 29 kg load at 45 C



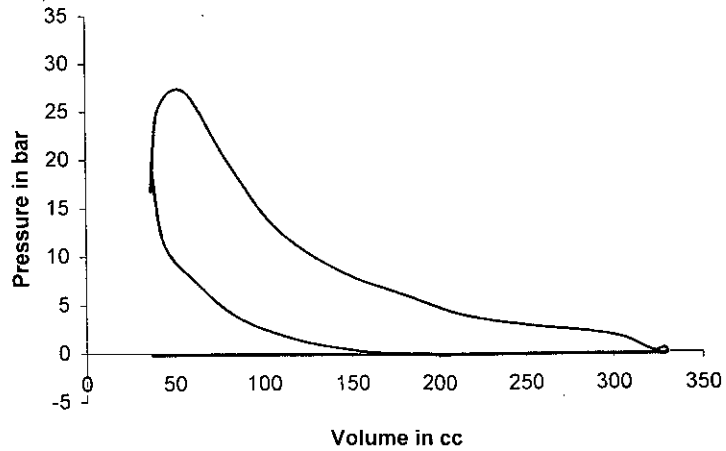
P-V Diagram at 2400 rpm and 29 kg load at 60 C



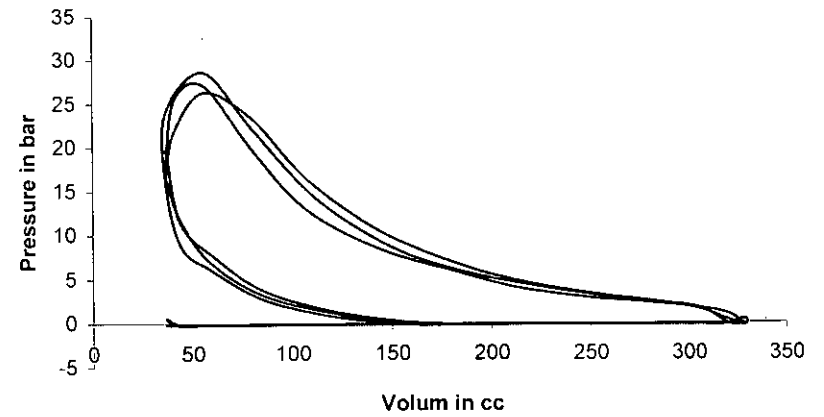
P-V Diagram at 2400 rpm and 29 kg load at 60 C



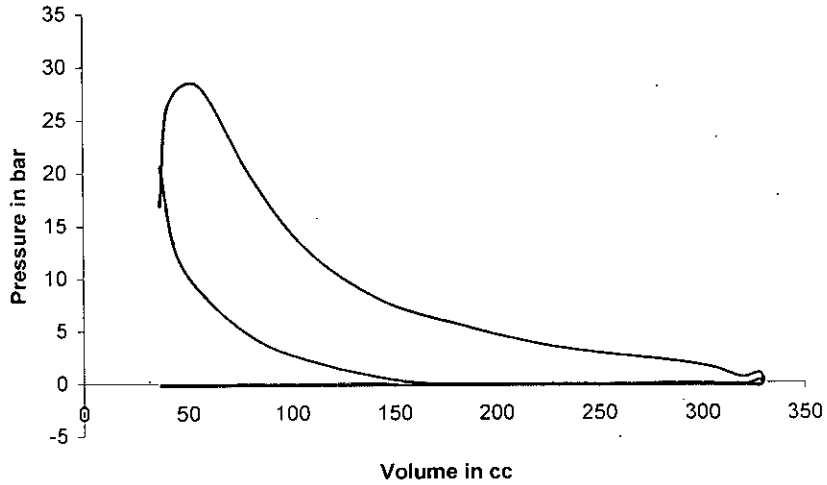
P-V Diagram at 2400 rpm and 29 kg load at 60 C



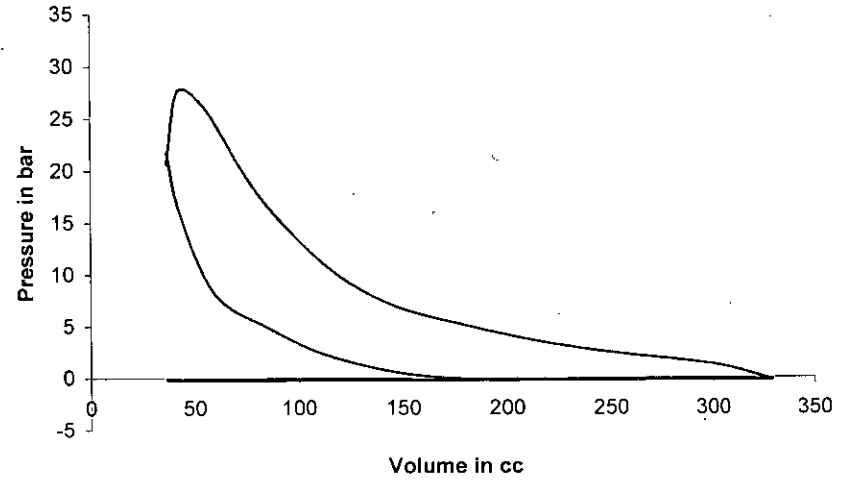
P-V Diagram at 2400 rpm and 29 kg load at 60 C



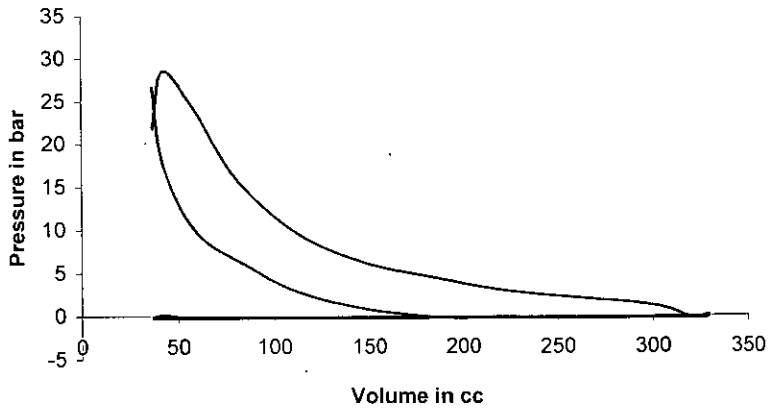
P-V Diagram at 2400 rpm and 29 kg load at 75 C



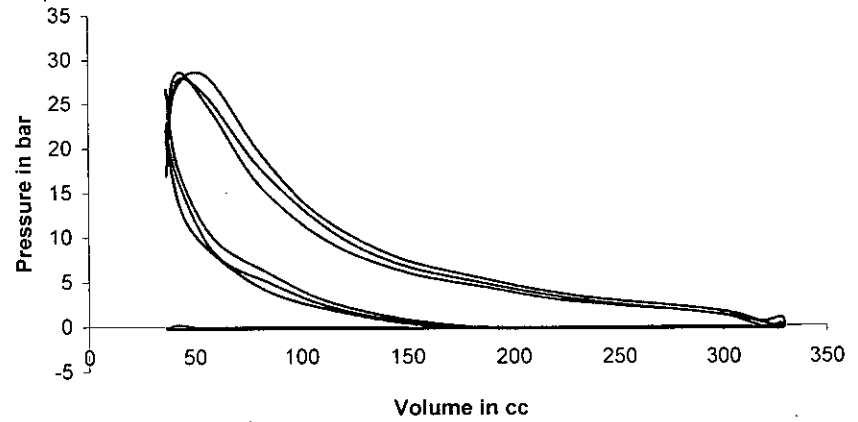
P-V Diagram at 2400 rpm and 29 kg load at 75 C



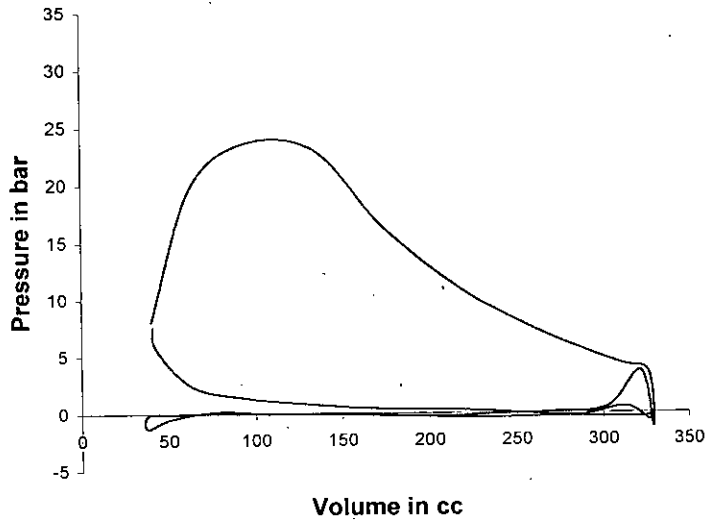
P-V Diagram at 2400 rpm and 29 kg load at 75 C



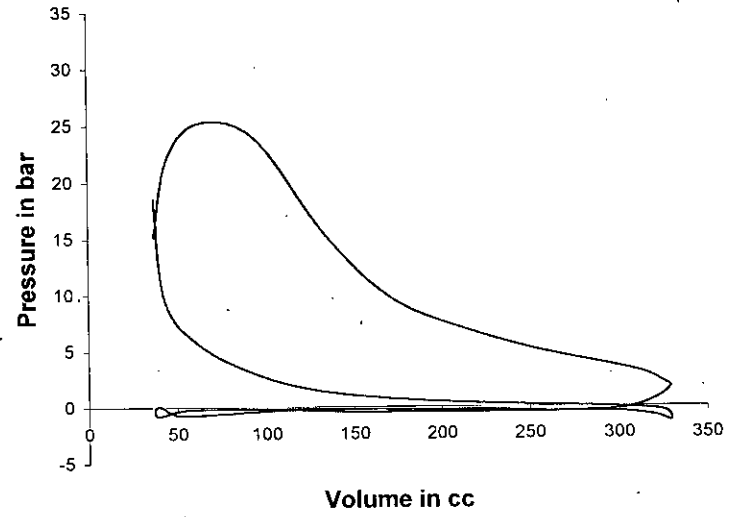
P-V Diagram at 2400 rpm and 29 kg load at 75 C



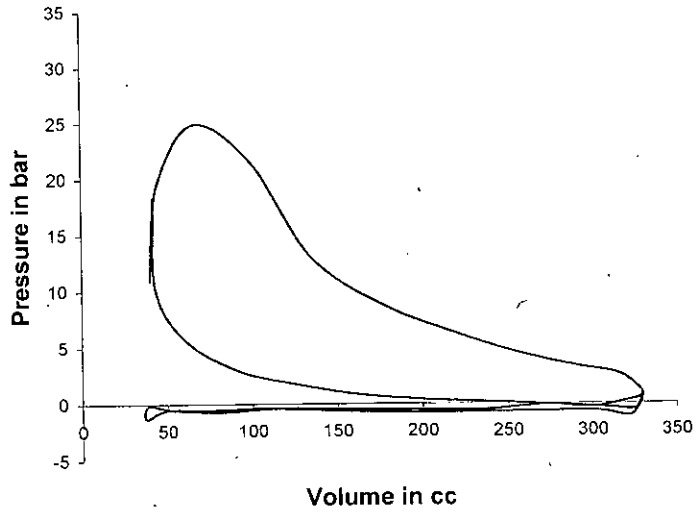
P-V Diagram at 2800 rpm and 29 kg load at 75 C



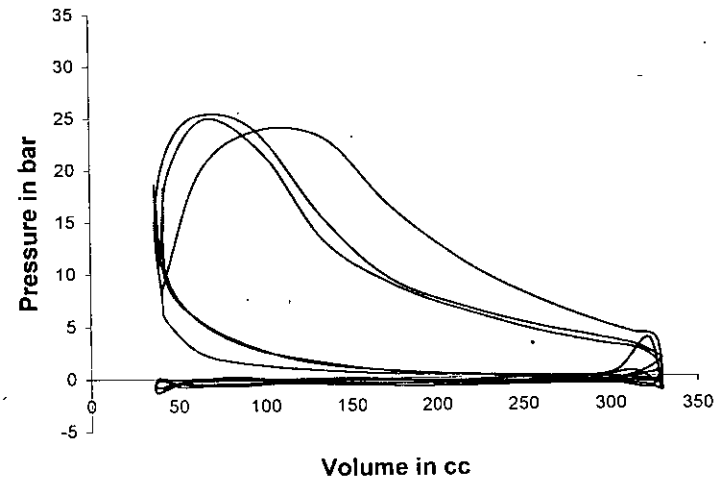
P-V Diagram at 2800 rpm and 29 kg load at 75 C



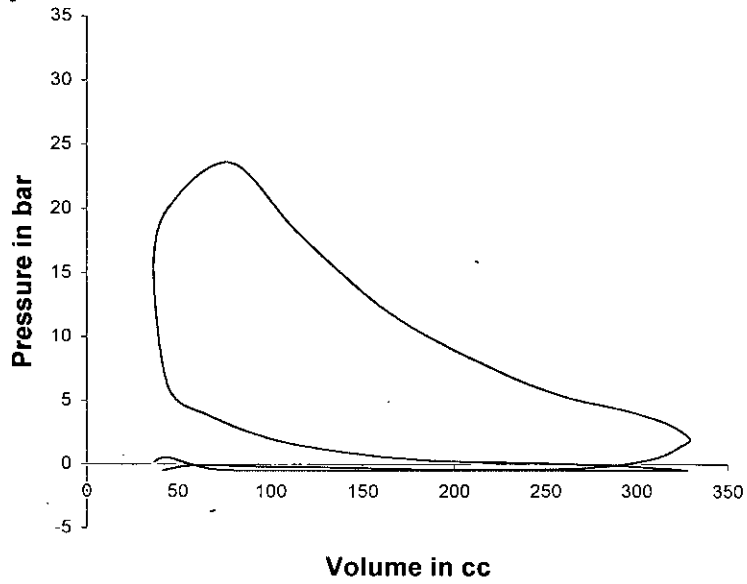
P-V Diagram at 2800 rpm and 29 kg load at 75 C



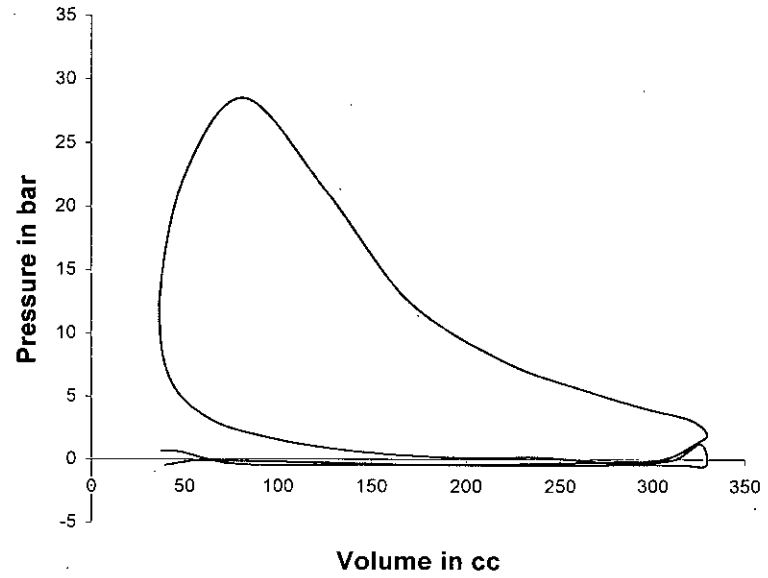
P-V Diagram at 2800 rpm and 29 kg load at 75 C



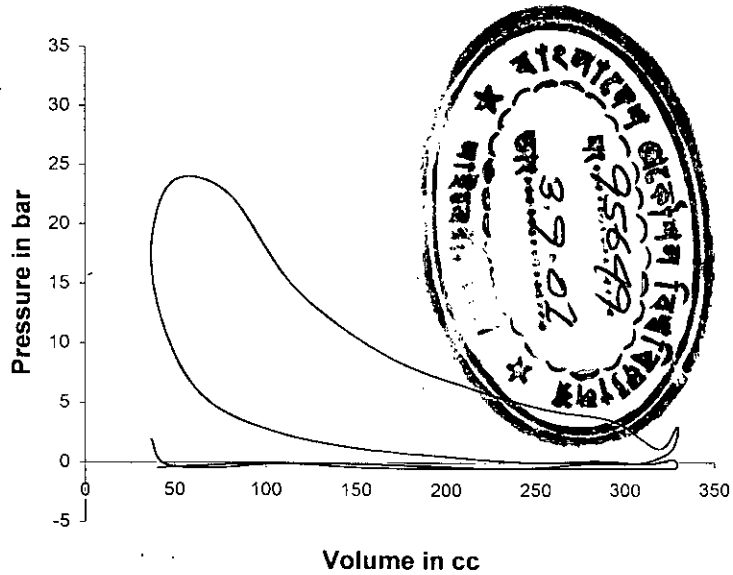
P-V Diagram at 3200 rpm and 26 kg load at 75 C



P-V Diagram at 3200 rpm and 26 kg load at 75 C



P-V Diagram at 3200 rpm and 26 kg load at 75 C



P-V Diagram at 3200 rpm and 26 kg load at 75 C

